Comparing the Use of Washingtonia Filifera Seed Extract in Various Solvents for ZnO Nanoparticle Synthesis, Characterization, and its Potential Anti-inflammatory and Biological Applications

Parwin Jalal Jalil
Soran University
Renjbar M. Mhamedsharif
Soran University
Bushra Hussain Shnawa
Soran University
Samir Mustafa Hamad
Soran University
Ahmed Salih Mohammed (ahmed.mohammed@univsul.edu.iq)
Soran University
Peyman K. Aspoukeh
Soran University

Research Article

Keywords: ZnONPs, Green synthesize, Anti-inflammatory, Anti-fungal, Anti-bacteria

Posted Date: October 19th, 2023

DOI: https://doi.org/10.21203/rs.3.rs-3446342/v1

Additional Declarations: No competing interests reported.

Comparing the Use of Washingtonia Filifera Seed Extract in Various Solvents for ZnO Nanoparticle Synthesis, Characterization, and its Potential Anti-inflammatory and Biological Applications

Parwin Jalal Jalil[1], Renjbar M. Mhamedsharif[1], Bushra Hussain Shnawa[2], Samir Mustafa Hamad[1], Ahmed Salih Mohammed[3*], Peyman K. Aspoukeh[1].

[1] Scientific Research Centre, Soran University, Soran, Kurdistan Region, Iraq.
[2] Biology Department, Faculty of Science, Soran University, Soran, Kurdistan Region, Iraq.
[3] Department of Civil Engineering, College of Engineering, University of Sulaimani, Sulaimaniyah 46001, Kurdistan Region, Iraq, *Corrsponding author, +9647701588695, ahmed.mohammed@univsul.edu.iq

Abstract

The present study involves the green synthesis of zinc oxide nanoparticles ZnO NPs using three different solvents for plant extract of ethanol (EtOH), methanol (MeOH), and double distilled water (ddH_2O) in a method that is rapid, cost-effective, and environmentally friendly. The novelty of this study was creating ZnO NPs from *Washingtonia filifera* plant seed extract. Green fabricated ZnO NPs were characterized via UV–Vis spectroscopy, Fourier transform infrared (FT-IR), energy-dispersive spectroscopy (EDX), and X-ray diffraction (XRD). SEM data showed the efficacy of palm seed extract metabolites in fabricating spherical shape of ZnONPs, with an avarage size of 50, 71.6, and 81.6 nm for ddH_2O, EtOH, and MeOH Zn ONPs, respectively. FT-IR analysis showed varied absorption peaks related to fuctional group of plant extract and nanoparticle formation. Moreover, data analysis revealed that the antimicrobial activity against pathogenic Gram-positive and Gram-negative bacteria and fungi was dose-dependent and exhibited variable inhibition zone values.

In comparison to the plant extract alone, which provides minimum antimicrobial activity, the ZnO NPs prepared from this plant inhibit bacterial activity more efficiently. MeOH-ZnO NPs formed a maximum clear zones, 23.5 ± 0.3, 26.0 ± 0.3, and 19.8 ± 0.3 mm, at highest concentrations of 500 µg/ml against *S. aureus*, *P. aeruginosa*, *E. coli,* respectively. EtOH-ZnO NPs exhibit 82.2, 82.2, and 67.2 % of mycelial inhibition after 6 days of treatment with ZnO NPs for *A. niger, A. fumigatus* and *S. apiospermum*, respectively. Also, biosynthesized ZnO NPs showed a potent anti-inflammatory activity of were dose-dependent. The present anti-bacterial activities were increased as the NPs concentration increased. The *W. filifera*-mediated ZnO NPs showed strong antimicrobial activity against clinical pathogens compared to standard drugs. This suggests that

plant-based synthesis of NPs can be an excellent strategy for developing versatile and eco-friendly biomedical products.

Keywords: ZnONPs, Green synthesize, Anti-inflammatory, Anti-fungal, Anti-bacteria.

1. Introduction

Nanoscience is a comprehensive field concerned with the study and application of nanoscale materials, and it is increasing in popularity. Compared to their bulk counterparts, nanoparticles (NPs) exhibit new and improved qualities due to changes in their characteristics [1, 2]. This substance comprises of atoms arranged in various forms, including single-crystal, poly-crystal, and amorphous structure [3]. The physical, chemical, and mechanical properties of nanomaterials are largely controlled by the nanoparticles' size, shape, and surface morphology [4]. Metal nanoparticles are used in various appications, including antimicrobial activities, superparamagnetic materials, electrical and thermal resistivity [5, 6]. The synthesis of NPs carried out via physical and chemical techniques such as the sol-gel method, hydrothermal, laser ablation, microwave-supported synthesis and metal reduction using a variety of reducing agents, including sodium citrate, hydrazine hydrate, and sodium borohydride have limited their applicability due to the poisonous chemicals and hazardous environments used in the reduction and stabilization operations [7].

Fortunately, nanoparticle synthesis using green methods has become increasingly popular due to its effectiveness and simplicity in generating high-productivity materials. Green methods are known for their safety, affordability, cleanliness, and environmental friendliness [8]. The biological synthesis of nanoparticles stands out as it does not necessitate the use of hazardous and toxic compounds, high temperatures, or high pressures. Additionally, there is no need for external reducing, capping, and stabilizing agents [9].

Meanwhile, green-based synthesized ZnO NPs have been utilized in many biological applications including anti-inflammatory properties without having any negative effects [10], anti-cancer [11], anti-diabetic [12], anti-fungal [13] and anti-bacterial activities [14]. ZnO is classified as a chemical that is "generally recognized as safe" (GRAS) by the U.S. Food and Drug Administration (FDA) [15]. The green manufacturing of ZnO NPs using various plant extracts as reducing and capping agents is a novel method that has been established in several research [16, 17]. Plant extracts are superior for synthesizing NPs because they are absent of toxic compounds and provide essential

phytochemical substances as a reducing agents of metallic ions. The enzyme, protein, flavonoid, polysaccharide, and phenol present in the plant extract play a crucial role in the particle size reduction [18].

The palm family has a variety of plant species that are widely used as human food, some of which may also have pharmaceutical uses [19]. However, there are few studies on *Washingtonia* palms, a genus of the Coryphoideae subfamily with two species: *W. filifera* and *W. robusta*. The nutritional analysis of *W. filifera* fruits, including the seeds, revealed that they have more carbohydrates than proteins [20]. The seeds of *W. filifera* have been shown to contain substances that have anti-oxidant, butyrylcholinesterase, and xanthine oxidase inhibitory activities, which is interesting because they are an inedible part of the fruit and are typically discarded [21]. When it comes to phytochemicals, previous researchers have examined the anti-oxidant properties of the aerial part of *W. filifera* and reported the presence of eight known flavonoids, including different luteolin and C-glycosyl derivatives, as well as two newly described substances, luteolin 7-O-glucoside 400-sulfate and 8-hydroxyisoscoparin (i.e., 8-hydroxychrysoeriol 6-C-glucoside) [22]. As a novelty, the current study highlights the use of *W. filifera* plant seeds since, there is no research report on the use of this plant for the synthesis of ZnO NPs. Also, the present work aims to investigate the best plant seed extractions of *W. filarifia palm* as a substantial reducing and capping agent for ZnONPs fabrication that has been extracted by three different solvents of ethanol, methanol, and double distilled water, compare their characterizations and biological applications to investigate the antimicrobial effects of ZnO NPs against *E. coli, S. aureus, P. aerogonisoa, A. flavus, A. fumigatus,* and *S. apiospermum*. In addition to assess their anti-inflammatory activity in vitro to find the highly effective prepared ZnO NPs. The findings of the current study may help develop a new, efficient approach for controlling pathogenic microbes.

2. Materials and Methods

2.1. Chemical Materials

Sigma-Aldrich manufactured the chemical substances in the United States, including sodium hydroxide (NaOH) and zinc nitrate hexahydrate ($Zn(NO_3)_2.6H_2O$). Oxoid Ltd., Basingstoke, X3296 Hampshire, England, provided the Mueller-Hinton agar (Rashmi Diagnostics Private Limited), and Potato dextrose agar oxoid (Neogen Culture Media). All the chemicals and solvents were purchased directly from Merck without further purification. All preparation procedures for the experiments employed double-distilled water.

2.2. Plant sampling, Identification, and Extraction

A specialist collected and identified the seeds of the *Washingtonia filifera* plant. The plant seed was cleaned thoroughly with distilled water to eradicate dirt before drying in the shade for 3-4 days. A grinder was used to grind the dried seeds into a fine powder, which was stored in zip-mouth polyethylene bags in the shade for future use. An amount of 25 g powdered plant seed was added to 100 mL in 250 ml flasks containing different solvent systems to compare the effective solvents for the biosynthesizing of ZnO NPs - Thus, the lyophilized plant materials were extracted in double distilled water (ddH_2O, aqueous extract), ethanol (EtOH, ethanol extract), or methanol (MeOH, methanol extract), parafilmed and incubated at room temperature under continuous stirring in a shaker for 3 days. After filtration and centrifugation at 10000 rpm, the ethanol and methanol extracts were concentrated using a rotary evaporator under reduced pressure at 60–70 ºC.

2.3. Phyto-mediated Synthesis of ZnONPs

To make the green fabricated ZnO NPs, 30 mL of plant seed extracted from ethanol, methanol, and double distilled water were mixed with 50 mL of 1 gm zinc nitrate $Zn(NO_3)_2$_$6H_2O$ for 40 minutes at 70 ˚C while the mixture was being stirred. The pH was brought to a 12 pH level by adding 1M sodium hydroxide (NaOH). The color of the final mixture was altered to a dark color due to the interaction between plant phytochemicals and metal salts, and creation of a colloidal suspension following the nucleation of ZnO NPs, as demonstrated by the UV-Vis technique. The Super Aquarius Cecil CE9500 UV/VIS dual-beam spectroscopy was used to study this nanoparticle production. After being centrifuged at 6000 rpm for 30 minutes to separate the sediment, the solid powder was cleaned twice with distilled water and then with methanol to remove contaminants and pollutants. Figure 1, shows the synthesis of ZnO NPs using freshly obtained *Washington* leaf extract by three different solvents.

2.4. Green fabricated ZnO NPs Characterizations

ZnO NPs were biosynthesized by the three different extracted solvents of the *W. filarifia* palm seeds and characterized by several analytical analyses. The formation of ZnO NPs confirmed the formation of ZnO NPs–Vis double-beam spectrophotometer (Super Aquarius). It was scanned from 200–850 nm wavelengths. Field emission scanning electron microscopy (FESEM) (Quanta 4500) was used to inspect the morphology of the obtained nanoparticles. The chemical

composition of the prepared nanostructures was measured by EDX (energy-dispersive X-ray spectroscopy) performed in FESEM. The X-ray diffraction (XRD) analysis was achieved by a PANanalytical X' Pert PRO (Cu Kα = 1.5406 A) with a scanning rate of 1°/min in the 2θ range from 20 to 80°. Additionally, particle size was calculated by the Debye–Scherrer equation. Also, FTIR accomplished further nanoparticle characterization.

2.5. Antimicrobial activities of ZnONPs

2.5.1. Anti-bacterial activities

The microorganisms were obtained from the Scientific Research Center that was previously used by Mhammedsharif et al. Mhammedsharif, Kolo [23]. Antimicrobial activity was investigated using the agar well diffusion method [24]. Muller-Hinton agar medium was prepared in Petri dishes, and bacterial cultures were swabbed on the test media with sterilized cotton swabs. The in vitro effects of ddH_2O, EtOH, and MeOH-ZnO NPs were evaluated in five concentrations (100, 200, 300, 400, and 500 ug/ml). A careful preparation was made to create 5 wells (6 mm) that were filled with 50 ul of various studied concentrations of ZnO NPs in addition to control well distilled wter were used. The plates were then incubated for 24 hours at 37 °C. The widths of the inhibition zones in (mm) were used for assessing the anti-bacterial activity of the biosynthesized ZnO NPs after incubation.

2.5.2. 1. Anti-fungal activities

Three pathogenic fungi, including *A. flavus*, *A. fumigatus* and *S. apiospermum*, were obtained from the leachate sample isolated, cultured, and purified from a previous study by Muksy and Kolo [25]. The purified fungi were cultured on PDA at 25 °C. The anti-fungal activity was performed by the agar well diffusion method. For this experiment, the autoclaved PDA media mixed with ZnO NPs at 50 ug/ml concentrations and a NP-free solution were poured into the Petri dishes (9 cm diameter). The fungi were inoculated after the PDA media solidified. A disc of 1 cm in diameter of mycelial material was taken from the edge of 7 day fungal old cultures and placed in the center of each Petri dish. The plates with the inoculums were then incubated at 25 °C. The efficacy of ZnO NPs treatment was evaluated at the time intervals of 1, 2, 3, 4, 5, and 6, days by measuring the diameter of fungal colonies. All tests were performed in triplicate, and the values were expressed in centimeters. The inhibition percentage was measured with the help of the mean colony diameter and computed according to the following equation formula (1) [26]

$$Growth\ inhibiton\ \% = \frac{C-T}{C} \times 100 \quad \ldots\ldots\ldots\ldots\ldots\ldots\ 1$$

Where (C) is the average mycelial growth of the control sample, and (T) is the average mycelial growth of the tested fungal sample.

2.5.2.2. Morphological assessment of fungal hyphae

To investigate the effect of ZnO NPs on preventing mycelial growth of the fungus under study. The mycelial growth and morphological alterations of *A. flavus, A. fumigatus,* and *S. apiospermum* were studied using SEM after treatment with ZnO NPs. Following in vitro evaluation of the examined ZnO NPs, the most effective form of biosynthesized ZnONPs confirmed by this study were used for SEM examination, which were EtOH-ZnONPs. Thus, mycelial material was cut from the edge of 6 days of experimental fungal cultures that were inoculated onto the PDA containing 50 µg EtOH-ZnO NPs and the control (the PDA containing no ZnO NPs) and dried in an oven at 37 ºC before being exposed to SEM analysis

2.5.3. Anti-inflammatory analysis of leaf extract and zinc oxide nanoparticles

The heat-induced hemolysis method was used to examine the effect of ZnO NPs on human red blood cells (HRBCs) in terms of their ability to reduce inflammation [27]. In brief, 5 mL of blood from a healthy volunteer was collected into an EDTA tube free of NSAIDS. The blood was then centrifuged at 3000 rpm for 20 minutes, and the supernatant was discarded. The pellet is centrifuged and washed three times with normal saline to get a clear supernatant. Then, a 10% suspension of HRBC pellets was produced using a normal saline solution.

In addition, 100 µl of diluted blood sample was mixed with 900 ml (20 µl distilled water (vehicle) and 800 µl PBS solution) for the control reaction mixtures. For the standard reaction activity, diclofenac sodium (10 mg/10 mL) was mixed in PBS (pH 7.4). Standard reaction mixtures included 100 µl of diluted blood sample and various studied concentrations of diclofenac sodium (DS) in PBS solution (10, 30, 50, 70, 90, and 110 µg/ml). The studied plant seed extract and prepared ZnO NPs prepared in PBS solution in the same concentrations were mixed with 100 microliters of diluted 10% blood suspension. Then, incubation at 54 °C for 30 min was followed by centrifugation at 5400 rpm for approximately 10 minutes for each test. Spectrophotometers were used to measure the absorbance of all samples.

The following equational formula (2) is used to calculate the percentage of inhibition of HRBC lysis:

$$Inhibition\ \% = \left[{AbsC - AbsT}/{AbsC} \right] \times 100 \quad \ldots\ldots\ldots\ldots\ldots\ldots 2$$

2.5.4. Statistical analysis

The data were compared using GraphPad Prism 8.02. All the experiments were conducted in triplicate. For data comparisons (ANOVA) test was used to determine the significance of differences between groups. *P*-values of < 0.05 were considered statistically significant.

3. Results and discussions

3.1. 1. Visual color observations and UV-Visible spectroscopy

Visual observation is the first essential indicator confirming synthesize of ZnO NPs synthesis. When the ($Zn(NO_3)_2.6H_2O$), added to the plant seed extract, the color of the extract was changed from light red to dark cream-colored precipitate as shown in Figure 1. Similar color changes of synthesized ZnONPs using *Hibiscus subdariffa* leaf extract, from light red to cream-colored precipitate, were displayed by Abdelbaky et al. Abdelbaky, Abd El-Mageed [28], confirming the growth of ZnO NPs.

Figure 2, represents the UV-Vis images of the plant extract absorption peaks around 270 and 300 nm (Figure 2 a). Additional peaks have been found for the plant extracted by ethanol and methanol solvents representing more phytochemical contents. Flavonoids are an essential class of secondary metabolites of plants that are abundant in plant-based foods [29]. A previous study reported the *W. filifera* reach of alkaloids and flavonoid content as the alcoholic preparations of *W. filifera* seeds were analyzed. B-type procyanidin dimers (B1-B4) were among the most abundant phenolic compounds in *W. filifera* seed extracts [21]. Also, three additional phenolic compounds, catechin, protocatechuic acid, and p-hydroxybenzoic acid, were identified [30].

Figure 2b, displays the maximum absorption peaks at 348 nm for the ddH_2O extract used for ZnO NPs synthesis and a wavelength of 350 and 370 nm for the MeOH and EtOH extract used for ZnO NPs synthesis, respectively. The peak appearance at this wavelength is due to the surface Plasmon absorption of ZnO NPs. The UV-Vis findings confirm the green synthesis of ZnO NPs. Previous study reports stated that ZnO NPs have peak values at the wavelengths 360–380 nm [31]. Also, the obtained findings were consistent with earlier studies by Senthilkumar et al. [32] examined the ability of *Tecona grandis* (L.) ALE to synthesize ZnO NPs with surface plasmon resonance (SPR) at 370 nm.

In addition, the energy bandgap of the prepared ZnO NPs is calculated by the Tauc equation $(ahv)^{1/n} = A(hv - Eg)$. As illustrated in Figure 2c, which verified the synthesis of ZnO NPs via *W. filarifia* seed extract. Where hυ is the photon energy (eV) related to the material, E_g is the band gap energy, A is the contradiction constant, and n is the exponential value of ½ for direct band gap energy [33]. Based on the fitting linear results in Figure 2c, the obtained band gap energy for ddH_2O-ZnO NPs, EtOH-ZnO NPs, and MeOH-ZnO NPs were 3.2, 3.1, and 2.8 Ev, respectively. The current band gap energy is in close agreement with previously reported values [34, 35]. The variation in E_g for the different ratios could be due to variation in the average crystal size of the NPs, as evidence of the quantum size effect.

3.1.2. X-ray Diffraction (XRD) Analysis of ZnO NPs

Figure 3, displays the green synthesized ZnO NPs pattern of XRD observed between 20° and 70°. The XRD pattern of biosynthesized ZnO NPs using seed extract of *W. filifera* from three solvents showed a strong diffraction peak. Generally, for all the three ZnO NPs, the XRD diffraction peaks existed at 2θ angles corresponding to the crystal lattice planes of (100), (002), (101), (102), (110), (103), (200), (112), and (201), respectively. These peaks are following those of (JCPDS card No: 98-006-512)**.** The narrow and sharp peaks of the XRD pattern confirmed that the biosynthesized ZnO NPs possessed a fine crystalline structure [36]. The average crystalline size of biosynthesized ZnO NPs was calculated using the Deby-Scherrer equation formula (3) [37]:

$$D = \frac{\beta \, Cos \, \theta}{k\lambda} \quad \ldots\ldots\ldots\ldots\ldots\ldots\ldots\ldots 3$$

The mean diameters of ddH_2O, MeOH, and EtOH-ZnO NPs produced by a green synthesis method are 23,6, 24,8, and 29,4 nm, respectively.

3.1.3. Scanning Electron Microscopy (SEM) Study

The scanning electron microscope (SEM) was utilized to examine the surface morphology, shape, and size of the prepared ZnO NPs. Figure 4, presents the three ZnO NPs formations along with their corresponding particle size distribution. It is evident from the figure that most of the ZnO NPs were spherical with fine distribution, and the ddH_2O nanoparticles size are distributed between 40 nm to 50 nm with a mean size of 50 nm. The mean sizes for EtOH-ZnO NPs and MeOH-ZnO NPs were 71 and 81 nm, respectively. The present part of the research confirmed that the average particle size of ZnO NPs formed by aqueous ddH_2O plant extract is smaller than that of ZnO NPs formed by the other two plant extract solvents. The variation in the size of NPs

probably due to the polarity effect of the solvent used for synthesis. The morphology of synthesized ZnO nanoparticles depends upon the precursor used, as determined by Zhang et al. and Medina et al. [38, 39]. Interaction occurs between the precursor used in the reaction and the solvent used in the synthesis, which can affect the size of ZnO nanoparticles. The polarity of solvents is a determining factor for the nucleation of ZnO nanocrystals and the crystal growth direction [40, 41].

3.1.4. Energy Dispersive X-ray Analysis (EDX) Spectrum of ZnO NPs

The energy-dispersive x-ray spectroscopy (EDX) spectrum was used to analyze the elemental composition of ZnO NPs produced from *W. filarifia* seed extracts. Figure 5**,** illustrates the pureness of ZnO NPs, thus verifying that the examined samples displayed the elemental peaks of zinc and oxygen. The EDX data confirms the presence of zinc and oxygen atoms in the three samples while exhibiting Zn and O peaks free of other impurities. According to the EDX analysis, the prepared ZnO NPs had a weight percentage of 80.4% -19.5%, 81.4% - 19%, and 86.5%, 13.4% of zinc and oxygen elements for ddH_2O-ZnONPs, EtOH-ZnONPs, and MeOH-ZnONPs, respectively. Thus, the presence and purity of the biosynthesized ZnONPs were more confirmed. The maximum peak values of Zn and O correspond well with the EDX results, indicating that the nanoparticles are stoichiometric and pure in their state.

3.1.5. FTIR Analysis of ZnONPs

The FTIR test is a technique that is used to identify the functional groups present in a sample by measuring the absorption of infrared radiation by the sample. The FTIR spectra of the ZnO NPs produced in different solvents show different peaks corresponding to the functional groups in the solvent molecules. In all three samples, a peak at around 3240-3397 cm^{-1} corresponds to the O-H stretching vibration of three different solvents [42]. For the ZnO nanoparticles produced in ethanol, the FTIR spectrum peaks at around 871 cm^{-1}, corresponding to the C-O stretching vibration of the ethanol molecule, and the stretching vibration of the C-C single bond appears at around 1063 cm^{-1}. The Zn-O stretching vibration appears at around 475 cm^{-1}. For the ZnO NPs produced in methanol, the FTIR spectrum peaks at around 880 cm -1, corresponding to the methanol molecule's C-O stretching vibration. The Zn-O stretching vibration may appear at around 491 cm^{-1}.it is important to mention that the exact position of Zn-O peaks may vary depending on the size and shape of the nanoparticles, as is shown in the Figure 6. For the ZnO NPs produced in waterThese results are consistence with a previous study conducted by Abbasi et al. [43]. The Zn-O stretching vibration is around 491 cm^{-1} [44]. It is important to mention that the exact position of Zn-O peaks may vary depending on the size and shape of the nanoparticles, as shown in Figure 6. According to Fakhari, Jamzad [45], zinc molecules in salt precursors and oxygen-containing functional groups in the seed extract of *W. filifera* led to the biosynthesis of ZnO NPs.

3.2. Estimation of antimicrobial activity

3.2.1. In vitro Anti-bacterial evaluation of *Washingtonia filifera* palm seed extract

Anti-bacterial activity of ddH_2O-PE, EtOH-PE, and MeOH-PE was compared through this work by adopting the agar well diffusion method. Additionally, the results indicated that the inhibitory effect of *W. filifera* seed extract increased as the extract concentration increased. Figures 7 and 8 show that the zone of inhibition of bacterial growth due to plant extract was formed. It can be observed that zinc nanoparticles prepared from water do not produce any zone with only a mild effect against *P. aeruginosa* at higher concentrations. However, the highest efficiency of ZnO NPs can be seen from methanol plant extract, which was 11.75±0.4, 12.3±0.4, and 12.7 ±0.3 for *E. coli, S. aureus*, and *P. aeruginosa,* respectively. The measurements of the inhibition zone for bacterial growth were also represented in Figures 7 and 8.

3.2.2. Anti-bacterial activities of ZnONPs

The potential biological use of green synthetic NPs as anti-bacterial agents has attracted biomedical interest [46]. In this context, the quantitative assessments of the anti-bacterial activity of ZnO NPs synthesized from palm seed extract were assessed against Gram-Positive *S. aureus*, Gram-negative *E. coli,* and *P. aeruginosa*. The examined bacteria were susceptible to the ZnO NPs in varying degrees, and these effects were dose-dependent. As can be observed from the macroscopic images in Figure 9 , ZnO NPs were more effective against *E. coli* and *S. aureus* than *P. aeroginosa*. The nanoparticle prepared from methanol plant extract exhibited the maximum zone of inhibition for *E. coli* (23.5±0.7 mm), *S. aureus* (26.0±0.3 mm), and *P. aeruginosa* (19.8 ±0.3) at 500 ug/ml ZnONPs and ddH_2O-ZnO NPs have the least effect on bacteria. This finding may be attributed to the fact that more plant phytochemicals will be released from methanol and ethanol solvents in comparison to aqueous extract Floris et al. [21] concluded that the total phenolic content in the aqueous extracts showed lower anti-oxidant capacity than the alcoholic extracts. The presence of proanthocyanidins with (epi)afzelechin units and A-type links. B-type procyanidin dimers (B1–B4) were among the major phenolic compounds in the preparations of *W. filifera* seeds that were reported in a previous study to have diverse biological activity [47, 48]. Figure 10 illustrates these results. The study outcome were in consistent with the findings of Gunalan et al. [49], who stated that increasing the ZnO NPs concentration in discs and wells consistently increased the growth inhibition due to optimal NPs diffusion in the agar medium**.**

Some hypothesized researchers have brought up bactericidal processes to explain the impact of ZnO NPs. Some researchers speculated that the liberated Zn from ZnO NPs has harmful characteristics that prevent several bacterial cell functions, like bacterial metabolism and enzyme activity, leading to bacterial cell death [50]. The other proposed mechanism is creating reactive oxygen species (ROS), which triggers oxidative stress and ultimately results in cell death [51, 52]. Another possibility is that ZnO nanoparticles induce mortality by attaching to bacterial cell membranes, accumulating inside the cytoplasm, and compromising the integrity of the membranes. This causes the contents of the cells to leak out, inducing cell death [53]. In general, the mechanisms underlying the interaction between bacteria and NPs involve the formation of extremely active hydroxyls and the deposition of NPs on the bacteria surface, with NPs accumulating in the cytoplasm or periplasmic region of the bacteria cell, thereby disrupting cellular operations and disorganizing the membrane. In *E. coli*, ZnO NPs disorganize the membrane and

penetrate the cytoplasm. The NPs neutralize respiratory enzymes and increase the emersion of cytoplasmic contents outward, which impairs the membrane and kills *E. coli* bacteria, creating a zone of bacterial growth inhibition around themselves [54, 55]

3.3. Anti-fungal activities of ZnONPs

3.3.1. Macroscopic evaluations of anti-fungal activities of ZnONPs

Figures 11,12 and 13 show the effect of ZnO NPs produced from different solvent extracts of *Washingtonia* seed on the growth of *A. flavus*, *A. fumigatus* and *S. apiospermum* in an in vitro model. The macroscopic images of the mycelial growth inhibitory effects of ZnO NPs against the studied fungi show that the fungal growth inhibition rate intensified with increasing NP concentration. Increasing the ZnO NP concentration from 100 to 500 ug/ml enhanced the treatment efficacy. Generally, the efficiency of ZnONPs against fungal species was in the order of EtOH-ZnO NPs> MeOH-ZnO NPs> ddH_2O-ZnO NPs. However, EtOH-ZnO NPs suspension was statistically significant in inhibiting fungal growth for all studied species, *p*-value <0.05. Compared to the control fungi growth after 6 days, there was a significant inhibition growth of *A. fumigatus* using EtOH-ZnO and MeOH-ZnO nanoparticles (p value<0.05), whereas the rate of growth inhibition for ddH_2O-ZnONPs was non-significant (p >0.05).

Highly significant growth inhibition can be found for both *A. flavus* and S. *apiospermum*. ZnONPs infused with the media inhibited the growth of *S. apiospermum* fungi more effectively than *A. fumigatus* and *A. flavus*. Further, the percentage inhibition of fungal growth was recorded in Table 1. The maximum percentage of mycelial growth inhibition of E-ZnO NPs was 82.2% for *A. flavus* in day 6, while for *A. fumigatus* the efficiency of ZnO NPs decreased from 92.1 in day 5 followed by 82.2 % in day 6. Compared with ddH_2O-ZnON Ps the lowest effect of ZnONPs can be detected by 11.0, 13.3, and 53.3 % for *A. flavus, A. fumigatus,* and *S. apiospermum,* respectively. The highly efficient inhibition of fungal growth also supported the fact that ZnO NPs were uniformly dispersed in PDA, which was proven by consistent inhibition results in this study Rajiv et al. [56] synthesized ZnO nanoparticles from the leaf extract of Parthenium hysterophorus. They explored their anti-fungal activity against *A. flavus* and *A. niger*, showing that ZnO NPs are good anti-fungal agents, inhibiting these phyto pathogens. However, the differences between the three fungi growth morphologies might be what causes their various anti-fungal effects. The innate tolerance of each fungus to ZnO NPs is another potential explanation for the differences [57].

3.3.2. Morphological investigations of fungal growth

To investigate the structural and growth changes of fungal samples after ZnO NPs treatment of *A. flavus, A. fumigatus* and *S. apiospermum*, SEM analysis was employed. This study chose the most efficient kind of the formed ZnO NPs against the studied fungi for morphology analysis. Figure 15 shows the images of mycelia obtained from the edges of each of the three studied fungal species treated with EtOH-ZnO NPs and cultured in the control (untreated samples). It can be demonstrated in untreated, actively growing mycelia, a typical net of fungal hyphae structure and a smooth surface in control fungal samples. All the conidia and hyphae-like structures remained intact and displayed a linear shape. Also, this finding was further confirmed by SEM analysis in Figure 16. After treatment with 50 µg of ZnO NPs, the hyphae lost their smoothness, more obviously it can be seen in *S. apiospermum*, indicating that ZnO NPs inhibited the growth of *S. apiospermum* by deforming the structure of fungal hyphae and the absence of fungal conidia reflecting inhibiting germinations of fungal conidia.

SEM observations of external mycelia from *A. fumigatus* and S. *apiospermum* colonies showed branched conidia with round and chain-like structures in the untreated sample. After treatment with 50 µg ZnO NPs for 6 days, germination of *A. fumigatus* conidia was inhibited, and conidial development was suppressed significantly, as seen in treatment images from Figure 16. These results suggest that ZnO NPs distorted and damaged the conidia of these two fungus. Consequently, the fungal growth was greatly inhibited. Similar results were observed by He et al. [58]; ZnO NPs caused deformation in fungal hyphae. In comparison, ZnO NPs prevented the development of conidiophores and conidia of *P. expansum*, eventually leading to the death of fungal hyphae.

However, for *A. flavus*, SEM images show no notable effect of ZnO NPs against this fungal growth. It can be seen that the number of conidial growth was greater in the control group in comparison with the treatment group.

The mechanism of anti-fungal activity of biogenic ZnO NPs was previously reported in the literature to involve their entry into the fungal cell via diffusion and endocytosis, followed by interference with the mitochondria in the cytoplasm and the subsequent release of reactive oxygen species and Zn^{2+} ions [59]. These Zn2+ ions passed through the fungal membrane and interacted with cellular DNA, causing nuclear damage, including persistent chromosomal damage, and, ultimately, inducing cell death [60]. According to previous research, the antimicrobial efficacy of

ZnO nanoparticles can be attributed to the production of reactive oxygen species (ROS) [61]. Reactive oxygen species, such as hydrogen peroxide (H_2O_2), superoxide (O_2), and hydroxyl radical (OH), induce oxidative stress damage, which leads to the disruption of cellular membranes, cellular proteins, and nucleic acids, and ultimately the induction of fungal cell death [62].

3.4. Estimation of Anti-inflammatory Activity of Zinc Oxide Nanoparticles

Inflammation is a natural response induced by the body's immune system in response to various bacteria, irritants, damaged cells, and potentially harmful stimuli. Many secondary metabolites and metallic nanoparticles have anti-inflammatory characteristics that have been proven both in vitro and in vivo [27]. From the results obtained in Figure 17, the ZnO NPs and *W.filifera* plant seed extract have an anti-inflammatory effect that is concentration-dependent, with the percentage of protection increasing as the concentration of the samples increases. At the concentration of 110 µg /mL, the ddH_2O-ZnO NPs produced 89.15% inhibition of RBC hemolysis, and the standard results achieved with standard indomethacin at the same concentrations were 91.3%, comparable to the results in Table 2.

In this study, effectiveness of ZnO NPs as an anti-inflammatory agent was evaluated in vitro through heat-induced hemolysis. This test's methodology is predicated on the stability and lysis of RBC membranes as the principle of investigation. With the help of RBC membrane lysis inhibition, the HRBC strength of studied plant extract was evaluated while the experiment was carried out at high temperatures. In light of the results obtained from anti-inflammatory activity, green synthesized zinc oxide nanoparticles are good anti-inflammatory agents. They can be very important sources in the therapeutic and pharmacological fields to alleviate various diseases.

The ZnO NPs and plant seed extract may stabilize the RBC membrane by preventing the release of active mediators of inflammation and lytic enzymes. Furthermore, many studies have revealed that plant flavonoids have anti-inflammatory and anti-oxidant activity [63, 64, 65]. Their anti-inflammatory properties are thought to be due to an inhibitory action on enzymes involved in synthesizing the chemical mediators of inflammation and arachidonic acid metabolism [66, 67]. During inflammation, lysosomes lyse and release their component enzymes, resulting in various disorders. Nonsteroidal anti-inflammatory drugs (NSAIDs) block lysosomal enzyme release or stabilize the lysosomal membrane [68]. When RBCs are exposed to harmful substances such as hypotonic medium or heat, the membranes lyse, resulting in hemolysis and hemoglobin oxidation [69]. Because the membranes of HRBCs are similar to those of lysosomes, the inhibition of

hypotonicity-induced RBCs membrane lysis was used to measure the mechanism of the anti-inflammatory effect of ZnO NPs and WFP.

4. Conclusions

Seed extracts of *W. filifera* in different solvents showed excellent potential as reducing agents in forming ZnONPs. Morphology, crystalstructural, and optical properites were studied using UV, FTIR, XRD, and SEM analysis confirmed the formation of ZnO NPs. The findings showed the purity and crystallinity of green synthesized ZnONPs. The patteren peaks of the XRD demonstrates the hexagonal crystal structures of the nanoparticles. On the nanoscale, ZnO NPs had a spherical shape, confirmed by the SEM pictures. The purity of ZnO nanoparticles and elemental composition was confirmed by EDX analysis. The FT-IR results showed that phytochemicals present in *W. filifera* are responsible for the reducing and capping of ZnO NPs. However, the size of ZnONPs produced by aqueous seed extract as smaller than ethanol and methanol seed extract solvents. Further, the anti-bacterial and anti-fungal activities of *W. filifera* plant seed extract alone and ZnONPs prepared from plant seed extracts were evaluated. Compared to ethanol, methanol, aqueous plant extract, and ddH_2O- ZnO NPs, the ZnO nanoparticles prepared from ethanol and methanol exhibited potent anti-bacterial and anti-fungal activities. Anti-bacterial analysis revealed that ZnO NPs synthesized from seed extracts exhibited significant inhibition capability against the clinical pathogens in the rate of efficiency MeOH> EtOH> ddH_2O ZnO NPs. Moreover, ethanol seed extract-prepared ZnO NPs provide the maximum anti-fungal activities while minimum anti-fungal inhibition percentages were seen by using ddH_2O-ZnO NPs against fungi. The anti-fungal findings were further investigated and supported by microscopic and SEM images of *A. flavus*, *A. fumigatus*, S. *apiospermum*. Tcontrary to antimicrobial findings, aqueous plant extract alone and with ZnONPs showed a potent anti-inflammatory activity. Overall, the synthesis of NPs using *W. filifera* in ethanol and methanol solvent extracts of *W .filifera* plant can have useful medicinal applications in the treatment of microbial pathogenies in comparison with standard drugs.

Availability of data and materials

The data supporting the conclusions of this article are included in the article.

Competing interests

None

Funding

No.

References

1. Bhardwaj A, Sharma G, Gupta S. Nanotechnology applications and synthesis of graphene as nanomaterial for nanoelectronics. Nanomaterials and Environmental Biotechnology. 2020:251-269.
2. Thakur S, Shandilya M, Guleria G. Appraisement of antimicrobial zinc oxide nanoparticles through Cannabis Jatropha curcasa Alovera and Tinosporacordifolia leaves by green synthesis process. Journal of Environmental Chemical Engineering. 2021;9(1):104882.
3. Gonçalves RA, Toledo RP, Joshi N, et al. Green synthesis and applications of ZnO and TiO2 nanostructures. Molecules. 2021;26(8):2236.
4. Raveendran P, Fu J, Wallen SLJJotACS. Completely "green" synthesis and stabilization of metal nanoparticles. 2003;125(46):13940-13941.
5. Awan S, Shahzadi K, Javad S, et al. A preliminary study of influence of zinc oxide nanoparticles on growth parameters of Brassica oleracea var italic. Journal of the Saudi Society of Agricultural Sciences. 2021;20(1):18-24.
6. Patino-Portela MC, Arciniegas-Grijalba PA, Mosquera-Sanchez LP, et al. Effect of method of synthesis on antifungal ability of ZnO nanoparticles: chemical route vs green route. Advances in nano research. 2021;10(2):191-210.
7. Salem SS, Fouda AJBter. Green synthesis of metallic nanoparticles and their prospective biotechnological applications: an overview. 2021;199:344-370.
8. Vijayaram S, Razafindralambo H, Sun Y-Z, et al. Applications of Green Synthesized Metal Nanoparticles — a Review. Biological Trace Element Research. 2023 2023/04/13. doi: 10.1007/s12011-023-03645-9.
9. Zhang D, Ma X-l, Gu Y, et al. Green synthesis of metallic nanoparticles and their potential applications to treat cancer. 2020;8.
10. Nagajyothi PC, Cha SJ, Yang IJ, et al. Antioxidant and anti-inflammatory activities of zinc oxide nanoparticles synthesized using Polygala tenuifolia root extract. 2015;146:10-17.

11. Naiel B, Fawzy M, Halmy MWA, et al. Green synthesis of zinc oxide nanoparticles using Sea Lavender (Limonium pruinosum L. Chaz.) extract: Characterization, evaluation of anti-skin cancer, antimicrobial and antioxidant potentials. 2022;12(1):20370.
12. Shaban EE, Abd El-Aziz ME, Ibrahim KS, et al. Effect of zinc oxide nanoparticles on diabetes development and complications in diabetic rats compared to conventional zinc sulfate and metformin. Biocatalysis and Agricultural Biotechnology. 2022 2022/11/01/;46:102538. doi: https://doi.org/10.1016/j.bcab.2022.102538.
13. Anum F, Jabeen K, Javad S, et al. Green synthesized silver nanoparticles as potent antifungal agent against Aspergillus terreus Thom. 2021;2021:1-10.
14. Shnawa BH, Mhammedsharif RM, Jalil PJ, et al. Antimicrobial activity of plant-extract-mediated synthesis of Silver-Zinc Oxide nanocomposites and their acaricidal efficacy on Hyalomma marginatum ticks. 2023:102765.
15. Espitia P, Otoni C, Soares N. Zinc oxide nanoparticles for food packaging applications. Antimicrobial food packaging: Elsevier; 2016. p. 425-431.
16. Berehu HM, Khan MI, Chakraborty R, et al. Cytotoxic potential of biogenic zinc oxide nanoparticles synthesized from swertia chirayita leaf extract on colorectal cancer cells. 2021;9:788527.
17. Shnawa BH, Jalil PJ, Aspoukeh P, et al. Protoscolicidal and Biocompatibility Properties of Biologically Fabricated Zinc Oxide Nanoparticles Using Ziziphus spina-christi Leaves. 2022;42(4).
18. Mittal A, Chisti YJA. andBanerjeeUC2013Biotechnol.31:346-56.
19. Geavlete P, Multescu R, Geavlete BJTaiu. Serenoa repens extract in the treatment of benign prostatic hyperplasia. 2011;3(4):193-198.
20. Nehdi IAJFC. Characteristics and composition of Washingtonia filifera (Linden ex André) H. Wendl. seed and seed oil. 2011;126(1):197-202.
21. Floris S, Fais A, Rosa A, et al. Phytochemical composition and the cholinesterase and xanthine oxidase inhibitory properties of seed extracts from the Washingtonia filifera palm fruit. 2019;9(37):21278-21287.
22. El-Sayed N, Ammar N, Al-Okbi S, et al. Antioxidant activity and two new flavonoids from Washingtonia filifera. 2006;20(1):57-61.

23. Mhammedsharif RM, Kolo KYJEM, Assessment. A case study of environmental pollution by pathogenic bacteria and metal (oid) s at Soran Landfill Site, Erbil, Iraqi Kurdistan Region. 2023;195(7):811.
24. Aldalbahi A, Alterary S, Ali Abdullrahman Almoghim R, et al. Greener synthesis of zinc oxide nanoparticles: Characterization and multifaceted applications. 2020;25(18):4198.
25. Muksy R, Kolo KJJoEE. Experimental Observations and Assessment of Landfill Leachate Bioremediation by Autochthonous Fungi Species and their Effective Geoactivities. 2023;24(1).
26. O'Rourke MJIMJ. 'Disease mongering'and the evidence. 2009;39(5):344-345.
27. Okoli CO, Akah PAJPB, Behavior. Mechanisms of the anti-inflammatory activity of the leaf extracts of Culcasia scandens P. Beauv (Araceae). 2004;79(3):473-481.
28. Abdelbaky AS, Abd El-Mageed TA, Babalghith AO, et al. Green synthesis and characterization of ZnO nanoparticles using Pelargonium odoratissimum (L.) aqueous leaf extract and their antioxidant, antibacterial and anti-inflammatory activities. 2022;11(8):1444.
29. Tresserra-Rimbau A, Lamuela-Raventos RM, Moreno JJJBP. Polyphenols, food and pharma. Current knowledge and directions for future research. 2018;156:186-195.
30. Floris S, Fais A, Medda R, et al. Washingtonia filifera seed extracts inhibit the islet amyloid polypeptide fibrils formations and α-amylase and α-glucosidase activity. 2021;36(1):517-524.
31. Kundu S, Sain S, Satpati B, et al. Structural interpretation, growth mechanism and optical properties of ZnO nanorods synthesized by a simple wet chemical route. 2015;5(29):23101-23113.
32. Senthilkumar N, Nandhakumar E, Priya P, et al. Synthesis of ZnO nanoparticles using leaf extract of Tectona grandis (L.) and their anti-bacterial, anti-arthritic, anti-oxidant and in vitro cytotoxicity activities. 2017;41(18):10347-10356.
33. Viezbicke BD, Patel S, Davis BE, et al. Evaluation of the Tauc method for optical absorption edge determination: ZnO thin films as a model system. 2015;252(8):1700-1710.
34. Fatimah I, Pradita RY, Nurfalinda AJPe. Plant extract mediated of ZnO nanoparticles by using ethanol extract of Mimosa pudica leaves and coffee powder. 2016;148:43-48.

35. Demissie MG, Sabir FK, Edossa GD, et al. Synthesis of Zinc Oxide Nanoparticles Using Leaf Extract of Lippia adoensis (Koseret) and Evaluation of Its Antibacterial Activity. Journal of Chemistry. 2020 2020/10/20;2020:7459042. doi: 10.1155/2020/7459042.
36. Vijayakumar S, Mahadevan S, Arulmozhi P, et al. Green synthesis of zinc oxide nanoparticles using Atalantia monophylla leaf extracts: Characterization and antimicrobial analysis. 2018;82:39-45.
37. Talam S, Karumuri SR, Gunnam NJISRN. Synthesis, characterization, and spectroscopic properties of ZnO nanoparticles. 2012;2012.
38. Zhang Y, Yu K, Jiang D, et al. Zinc oxide nanorod and nanowire for humidity sensor. 2005;242(1-2):212-217.
39. Medina J, Bolaños H, Mosquera-Sanchez LP, et al. Controlled synthesis of ZnO nanoparticles and evaluation of their toxicity in Mus musculus mice. International Nano Letters. 2018 2018/09/01;8(3):165-179. doi: 10.1007/s40089-018-0242-6.
40. Shi W, Cheng B, Zhang L, et al. Influence of excitation density on photoluminescence of zinc oxide with different morphologies and dimensions. 2005;98(8).
41. Lizandara-Pueyo C, van den Berg MW, De Toni A, et al. Nucleation and growth of ZnO in organic solvents-an in situ study. 2008;130(49):16601-16610.
42. Ilkhechi NN, Mozammel M, Khosroushahi AYJPB, et al. Antifungal effects of ZnO, TiO2 and ZnO-TiO2 nanostructures on Aspergillus flavus. 2021;176:104869.
43. Abbasi BA, Iqbal J, Ahmad R, et al. Bioactivities of Geranium wallichianum leaf extracts conjugated with zinc oxide nanoparticles. 2019;10(1):38.
44. Sahai A, Goswami NJPEL-dS, Nanostructures. Structural and vibrational properties of ZnO nanoparticles synthesized by the chemical precipitation method. 2014;58:130-137.
45. Fakhari S, Jamzad M, Kabiri Fard HJGcl, et al. Green synthesis of zinc oxide nanoparticles: a comparison. 2019;12(1):19-24.
46. Krishnamoorthy R, Athinarayanan J, Periyasamy VS, et al. Antibacterial Mechanisms of Zinc Oxide Nanoparticle against Bacterial Food Pathogens Resistant to Beta-Lactam Antibiotics. Molecules (Basel, Switzerland). 2022 Apr 12;27(8). doi: 10.3390/molecules27082489. PubMed PMID: 35458685; PubMed Central PMCID: PMCPMC9032754. eng.

47. Ling ZQ, Xie BJ, Yang EL. Isolation, characterization, and determination of antioxidative activity of oligomeric procyanidins from the seedpod of Nelumbo nucifera Gaertn. Journal of agricultural and food chemistry. 2005 Apr 6;53(7):2441-5. doi: 10.1021/jf040325p. PubMed PMID: 15796576; eng.
48. Ao C, Higa T, Ming H, et al. Isolation and identification of antioxidant and hyaluronidase inhibitory compounds from Ficus microcarpa L. fil. bark. Journal of Enzyme Inhibition and Medicinal Chemistry. 2010 2010/06/01;25(3):406-413. doi: 10.3109/14756360903213473.
49. Gunalan S, Sivaraj R, Rajendran VJPiNSMI. Green synthesized ZnO nanoparticles against bacterial and fungal pathogens. 2012;22(6):693-700.
50. Soren S, Kumar S, Mishra S, et al. Evaluation of antibacterial and antioxidant potential of the zinc oxide nanoparticles synthesized by aqueous and polyol method. 2018;119:145-151.
51. Agarwal H, Menon S, Kumar SV, et al. Mechanistic study on antibacterial action of zinc oxide nanoparticles synthesized using green route. 2018;286:60-70.
52. Mendes CR, Dilarri G, Forsan CF, et al. Antibacterial action and target mechanisms of zinc oxide nanoparticles against bacterial pathogens. Scientific reports. 2022 2022/02/16;12(1):2658. doi: 10.1038/s41598-022-06657-y.
53. Jayaseelan C, Rahuman AA, Kirthi AV, et al. Novel microbial route to synthesize ZnO nanoparticles using Aeromonas hydrophila and their activity against pathogenic bacteria and fungi. 2012;90:78-84.
54. Raghupathi KR, Koodali RT, Manna ACJL. Size-dependent bacterial growth inhibition and mechanism of antibacterial activity of zinc oxide nanoparticles. 2011;27(7):4020-4028.
55. Kairyte K, Kadys A, Luksiene ZJJoP, et al. Antibacterial and antifungal activity of photoactivated ZnO nanoparticles in suspension. 2013;128:78-84.
56. Rajiv P, Rajeshwari S, Venckatesh RJSAPAM, et al. Bio-Fabrication of zinc oxide nanoparticles using leaf extract of Parthenium hysterophorus L. and its size-dependent antifungal activity against plant fungal pathogens. 2013;112:384-387.

592 57. Berman J, Krysan DJ. Drug resistance and tolerance in fungi. Nature reviews
593 Microbiology. 2020 Jun;18(6):319-331. doi: 10.1038/s41579-019-0322-2. PubMed PMID:
594 32047294; PubMed Central PMCID: PMCPMC7231573. eng.
595 58. He L, Liu Y, Mustapha A, et al. Antifungal activity of zinc oxide nanoparticles against
596 Botrytis cinerea and Penicillium expansum. 2011;166(3):207-215.
597 59. Agarwal H, Rajeshkumar S, Shanmugam VK. Microbe-mediated synthesis of zinc oxide
598 nanoparticles. Zinc-Based Nanostructures for Environmental and Agricultural
599 Applications: Elsevier; 2021. p. 53-63.
600 60. Patra P, Mitra S, Debnath N, et al. Biochemical-, biophysical-, and microarray-based
601 antifungal evaluation of the buffer-mediated synthesized nano zinc oxide: an in vivo and
602 in vitro toxicity study. 2012;28(49):16966-16978.
603 61. Lipovsky A, Nitzan Y, Gedanken A, et al. Antifungal activity of ZnO nanoparticles—the
604 role of ROS mediated cell injury. 2011;22(10):105101.
605 62. Sharma S, Singh VK, Kumar A, et al. Effect of nanoparticles on oxidative damage and
606 antioxidant defense system in plants. 2019:315-333.
607 63. Middleton Jr E, Kandaswami CJBp. Effects of flavonoids on immune and inflammatory
608 cell functions. 1992;43(6):1167-1179.
609 64. Read MAJTAjop. Flavonoids: naturally occurring anti-inflammatory agents.
610 1995;147(2):235.
611 65. Halliwell B, Rafter J, Jenner AJTAjocn. Health promotion by flavonoids, tocopherols,
612 tocotrienols, and other phenols: direct or indirect effects? Antioxidant or not?
613 2005;81(1):268S-276S.
614 66. Owoyele VB, Oloriegbe YY, Balogun EA, et al. Analgesic and anti-inflammatory
615 properties of Nelsonia canescens leaf extract. 2005;99(1):153-156.
616 67. Metowogo K, Agbonon A, Eklu-Gadegbeku K, et al. Anti-ulcer and anti-inflammatory
617 effects of hydroalcohol extract of Aloe buettneri A. Berger (Lilliaceae). 2008;7(1):907-
618 912.
619 68. Mounnissamy VM, Kavimani S, Balu V, et al. Evaluation of Anti-inflammatory and
620 Membrane stabilizing property of Ethanol Extract of Cansjera rheedii J. Gmelin
621 (Opiliaceae). 2007;6(2):235-0.

69. Ferrali M, Signorini C, Ciccoli L, et al. Iron release and membrane damage in erythrocytes exposed to oxidizing agents, phenylhydrazine, divicine and isouramil. 1992;285(1):295-301.

627

628 **Table 1.** Screening of anti-fungal efficiency of the biogenic zinc oxide nanoparticles.

Treatment (cm)	*Aspergillus flavus*						*Aspergillus fumigatus*						*Scedosporium apiospermum*					
	4 days	%	5 days	%	6 days	%	4 days	%	5 days	%	6 days	%	4 days	%	5 days	%	6 days	%
DdH$_2$O-ZnO NPs	5.7	12.3	6.4	26.4	8	11.1	5.7	25	6.4	26.4	7.8	13.3	1	71.4	2.5	51.9	2.7	53.4
EtOH-ZnO NPs	1.6	75.3	1.7	80.4	1.6	82.2	1.6	78.9	1.7	92.1	1.6	82.2	0.8	77.1	1.2	76.9	1.9	67.2
MeOH-ZnO NPs	1.8	75.3	2.0	77.0	2.7	70	1.8	76.3	2.0	77.0	2.7	70	0	100	0	100	1	82.7
Control	6.5	0	8.7	0	9	0	7.6	0	8.7	0	9.0	0	3.5	0	5.2	0	5.8	0

629 **Note:** The data Means from three replicates were compared to the control group by ANOVA (Tukey test) were recommended, (p value <0.05) represents as
630 strongly significant (p value<0.0001) difference of treatment groups compared to the control group.

631 **Table 2.** Anti-inflammatory effects of ZnO NPs, *W.filifera* plant (WFP) seed extract, and standard drug.

Treatments (µg/ml)	Mean ±SD											
	10 µg/ml	%	30 µg/ml	%	50 µg/ml	%	70 µg/ml	%	90 µg/ml	%	110 µg/ml	%
DdH$_2$O-ZnO NPs	0.19± 0.01	77.1	0.182±0.01	78.072	0.203±0.03	75.54	0.156±0.01	81.2	0.138±0.01	83.37	0.09±0.01	89.15
EtOH-ZnO NPs	0.049± 0.0	40.24	0.384±0.05	53.73	0.299±0.01	63.97	0.267±0.01	67.83	0.223±0.2	73.13	0.191±0.01	76.9
MeOH-ZnO NPs	0.69± 0.01	16.8	0.65±0.08	21.68	0.56±0.04	32.53	0.53±0.04	36.14	0.46±0.01	44.57	0.41±0.06	50.6
WFP	0.45±0.0	45.78	0.345±0.04	58.43	0.293±0.01	64.69	0.187±0.0	77.46	0.136±0.06	83.61	0.097±0.0	88.3
D.S	0.21 ±0.01	74.69	0.195±0.01	76.5	0.142±0.01	82.89	0.103±0.0	87.59	0.079±0.01	90.48	0.067±0.0	91.92
Vehicle	0.83 ±0.01											

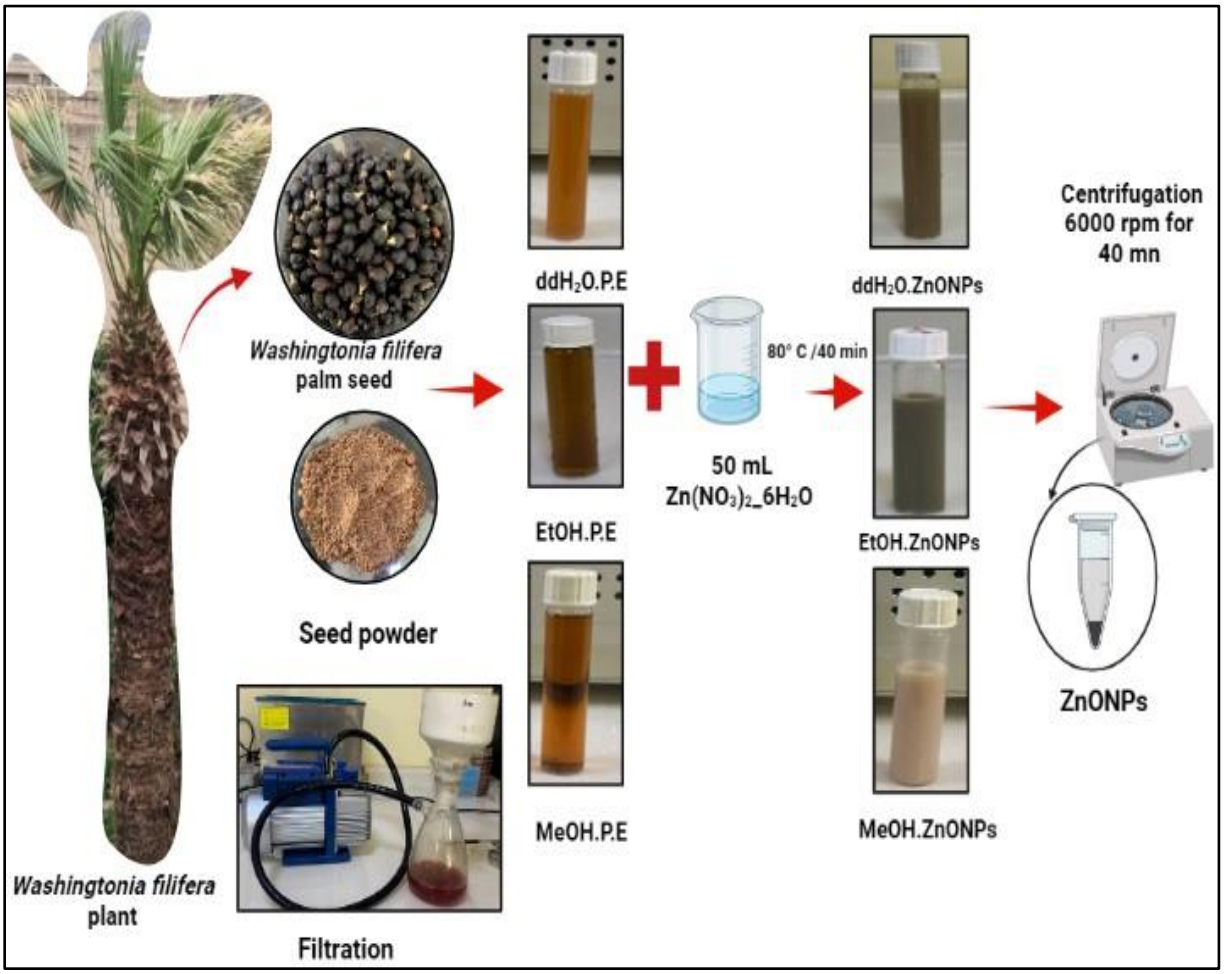

Figure 1. Schematic diagram of green synthesis of ZnONPs prepared by three different solvents of double distilled water (ddH_2O), ethanol (EtOH), and methanol (MeOH).

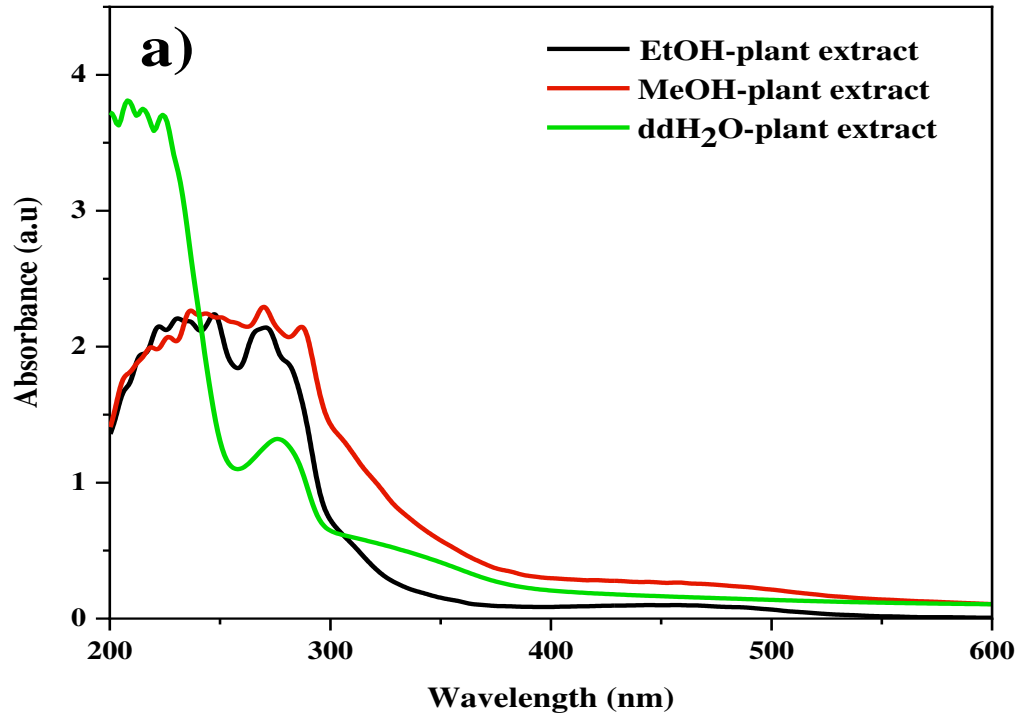
a)
EtOH-plant extract
MeOH-plant extract
ddH2O-plant extract
Absorbance (a.u)
Wavelength (nm)
0
1
2
3
4
200
300
400
500
600

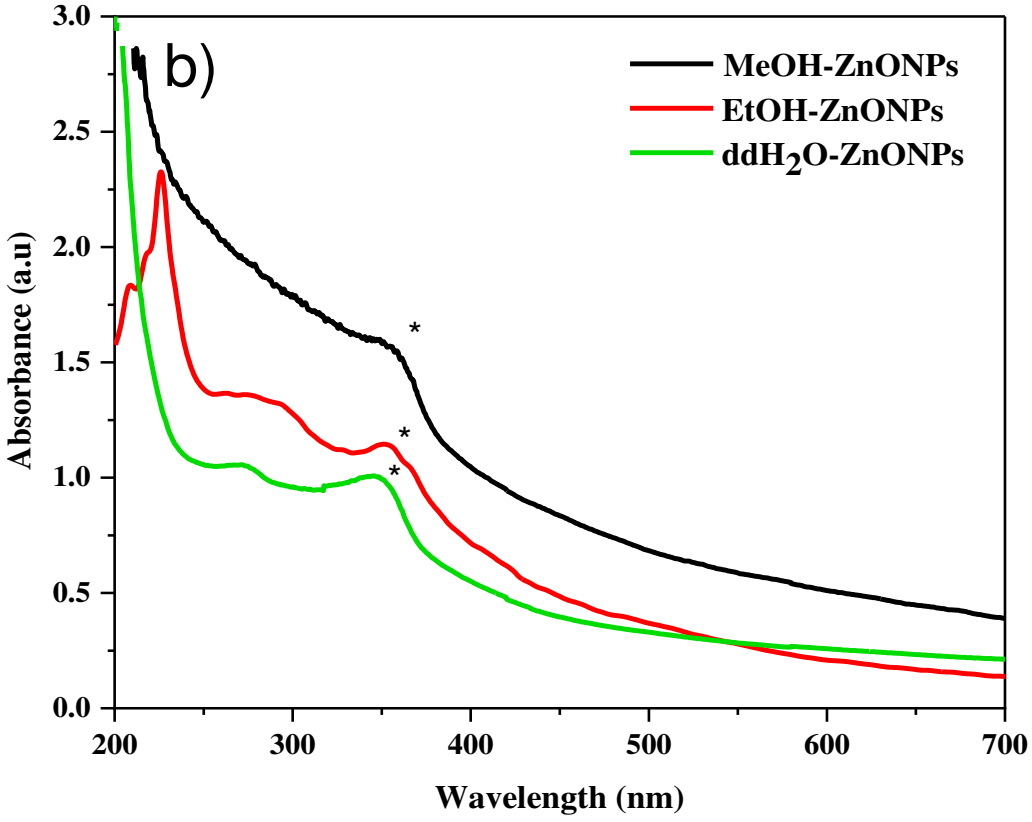
b)
MeOH-ZnONPs
EtOH-ZnONPs
ddH2O-ZnONPs
Absorbance (a.u)
Wavelength (nm)
0.0
0.5
1.0
1.5
2.0
2.5
3.0
200
300
400
500
600
700
*
*
*

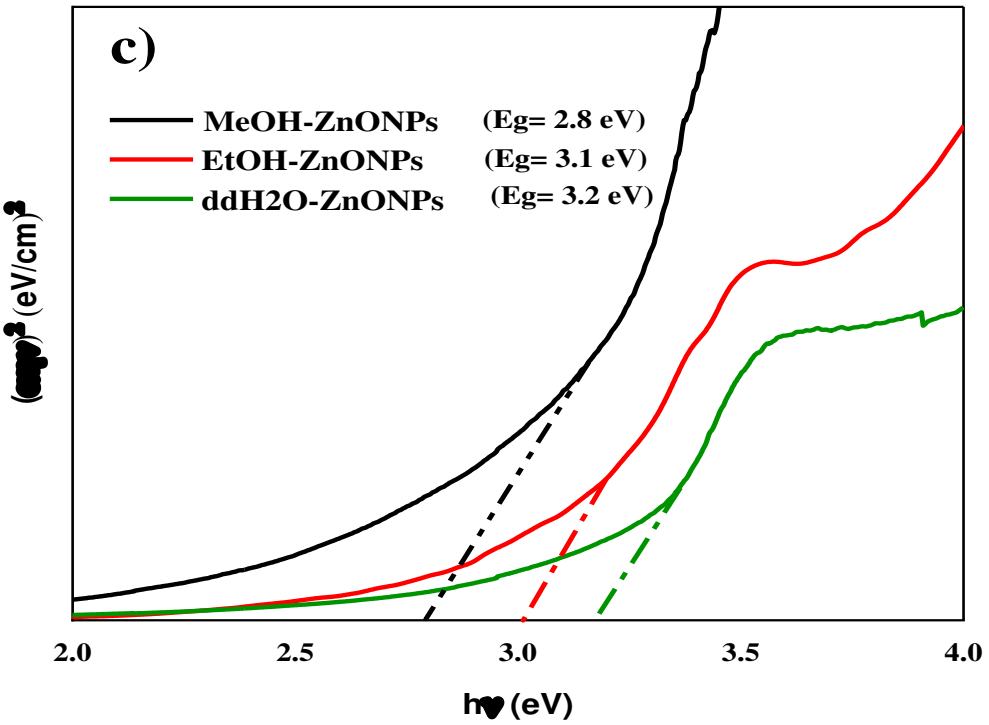

641

642 **Figure 2.** a) UV/Vis spectrum of *W. filarifia* seed extract by ddH_2O, ethanol, and methanol, b)
643 UV/Vis spectrum of ZnO NPs synthesized by three extracted *W. filarifia* seed plant, and c) Band
644 gap energy of the biosynthesized ZnO nanoparticles using the Tauc plot method.

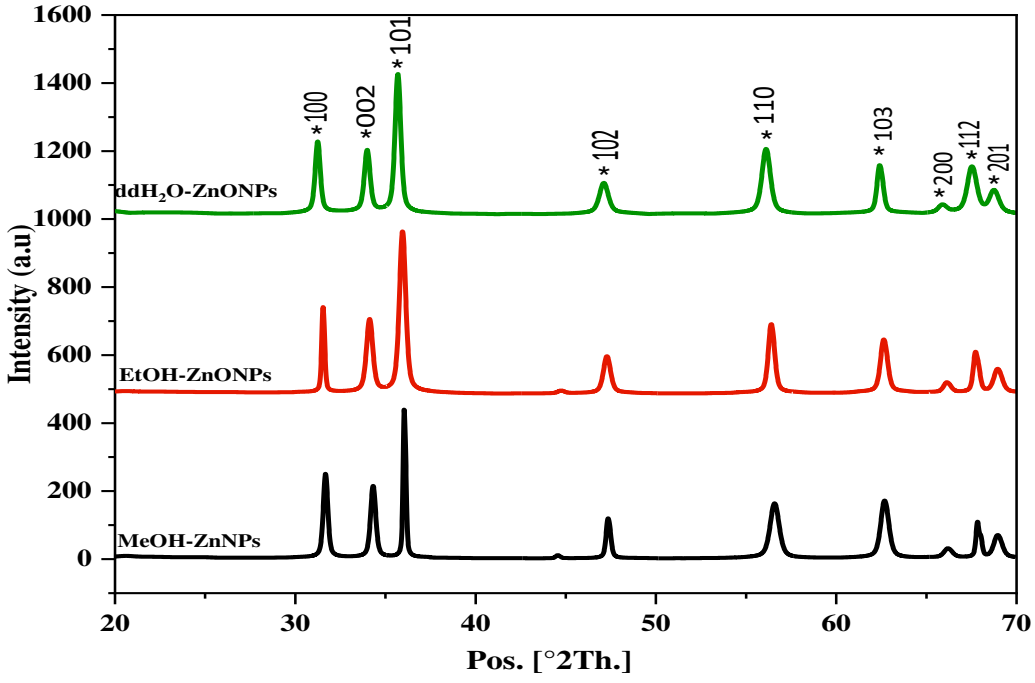

645

646 **Figure 3**. XRD pattern of ddH_2O-ZnO NPs; MeOH-ZnONPs; and EtOH-ZnONPs.

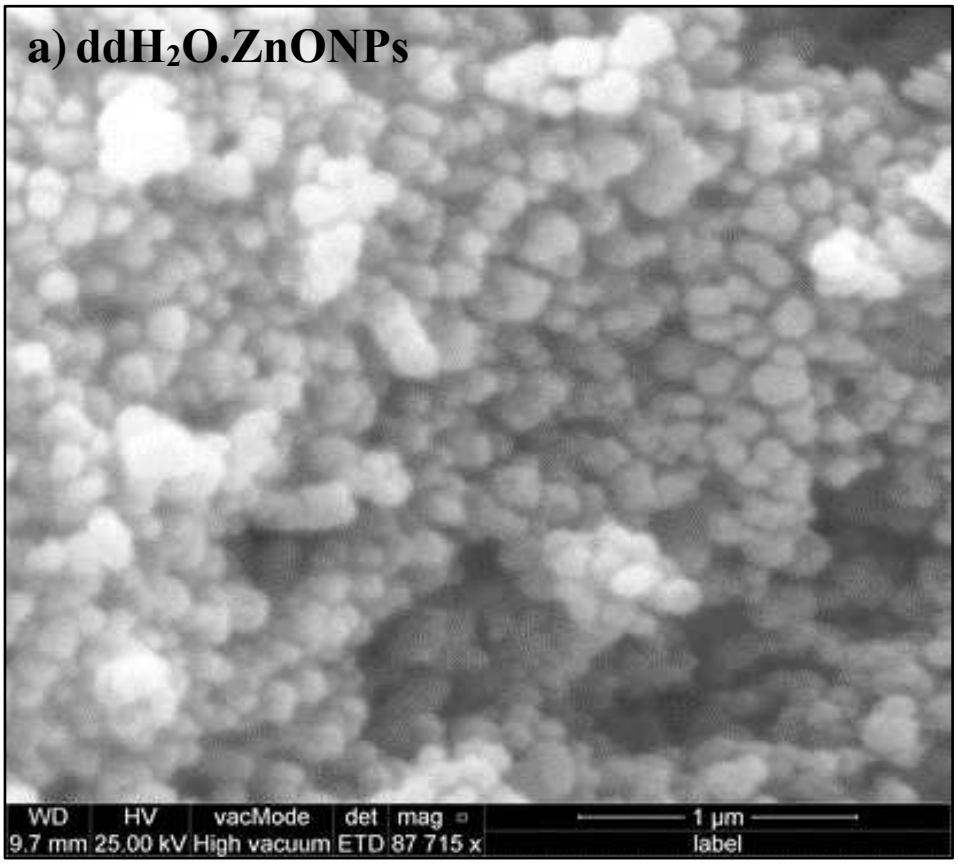
a) ddH2O.ZnONPs
WD HV vacMode det mag
9.7 mm 25.00 kV High vacuum ETD 87 715 x
1 µm
label

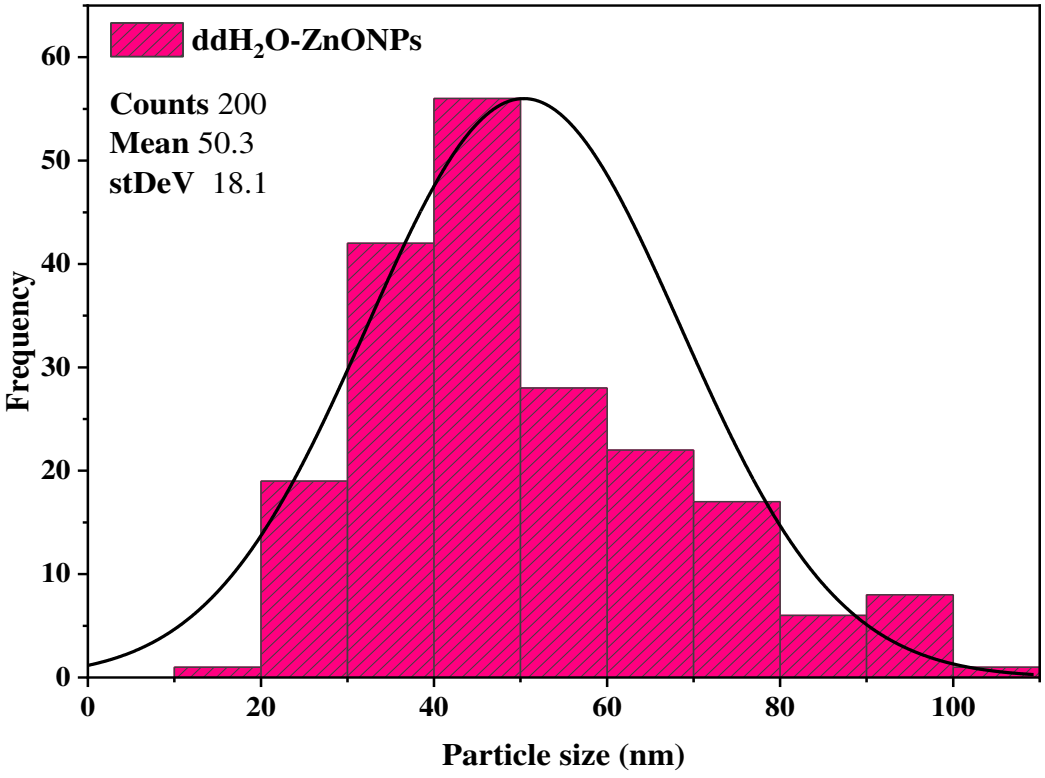
ddH2O-ZnONPs
Counts 200
Mean 50.3
stDeV 18.1
Frequency
Particle size (nm)
0
10
20
30
40
50
60
0
20
40
60
80
100

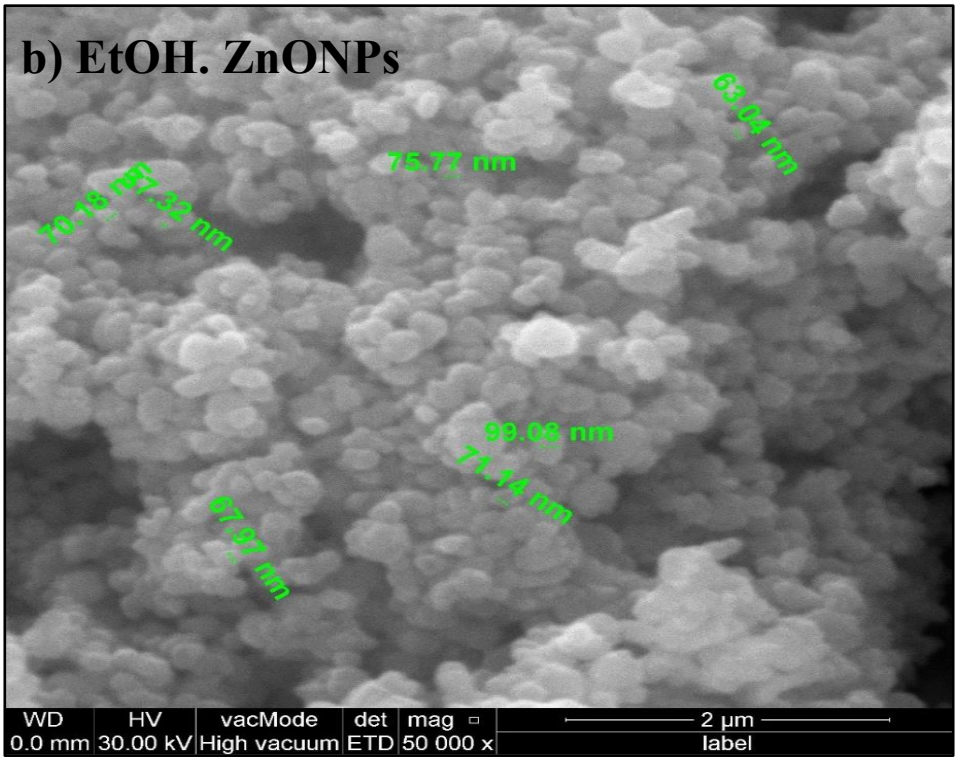
b) EtOH. ZnONPs
63.04 nm
75.77 nm
67.32 nm
70.18 nm
99.08 nm
71.14 nm
67.97 nm
WD
0.0 mm
HV
30.00 kV
vacMode
High vacuum
det
ETD
mag
50 000 x
2 µm
label

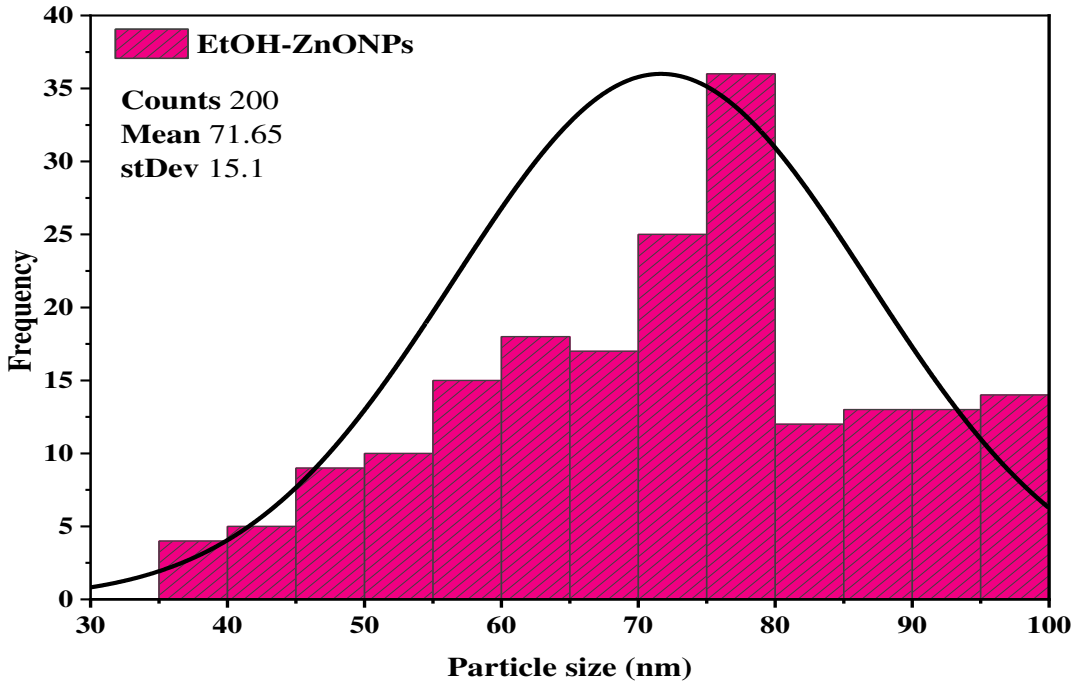
EtOH-ZnONPs
Counts 200
Mean 71.65
stDev 15.1
Frequency
Particle size (nm)
0
5
10
15
20
25
30
35
40
30
40
50
60
70
80
90
100

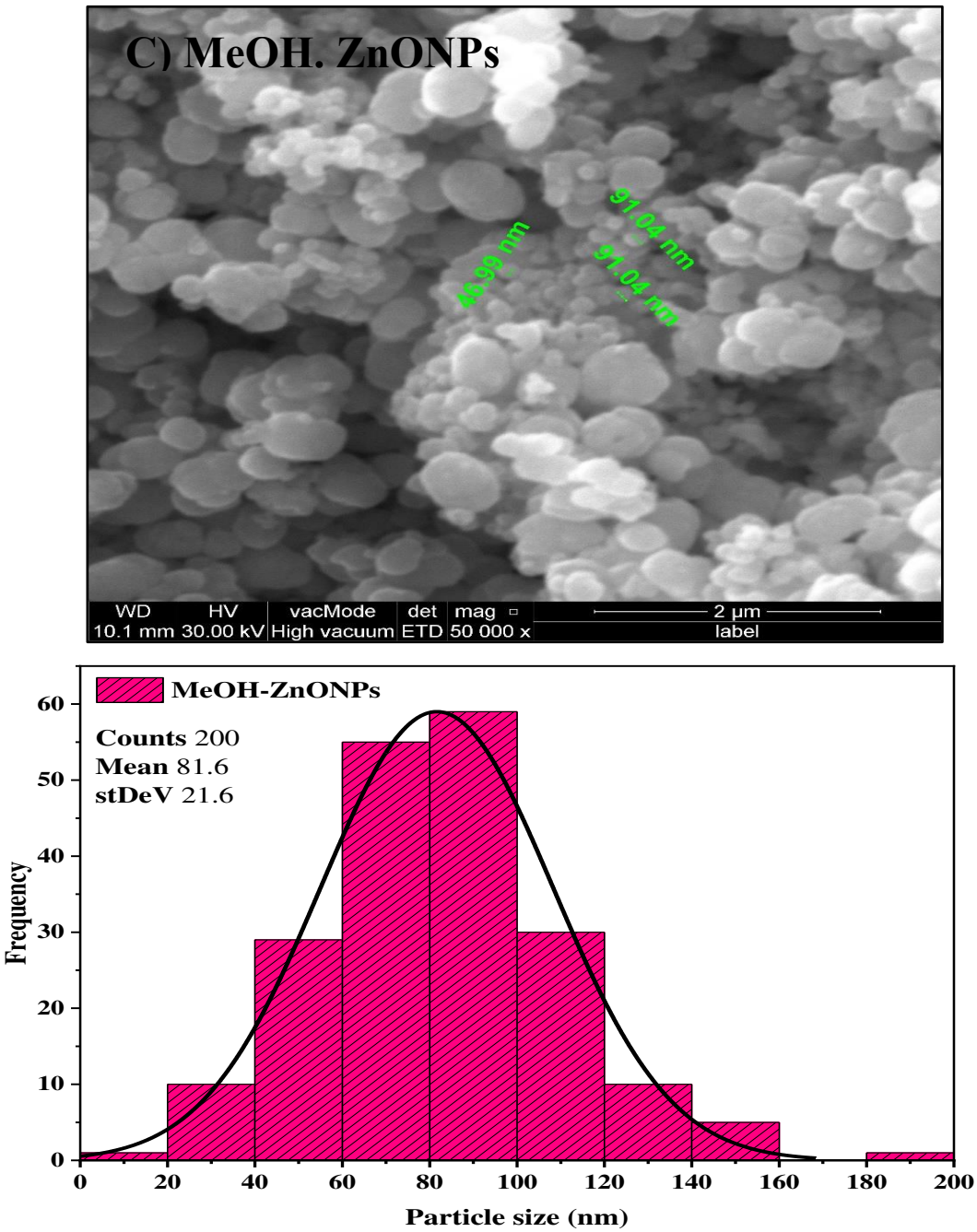

Figure 4. SEM analysis of the ZnO NPs synthesized by palm seed extracted by a) ddH_2O; b) EtOH; and c) MeOH solvents and particle size distribution of the zinc oxide nanoparticles.

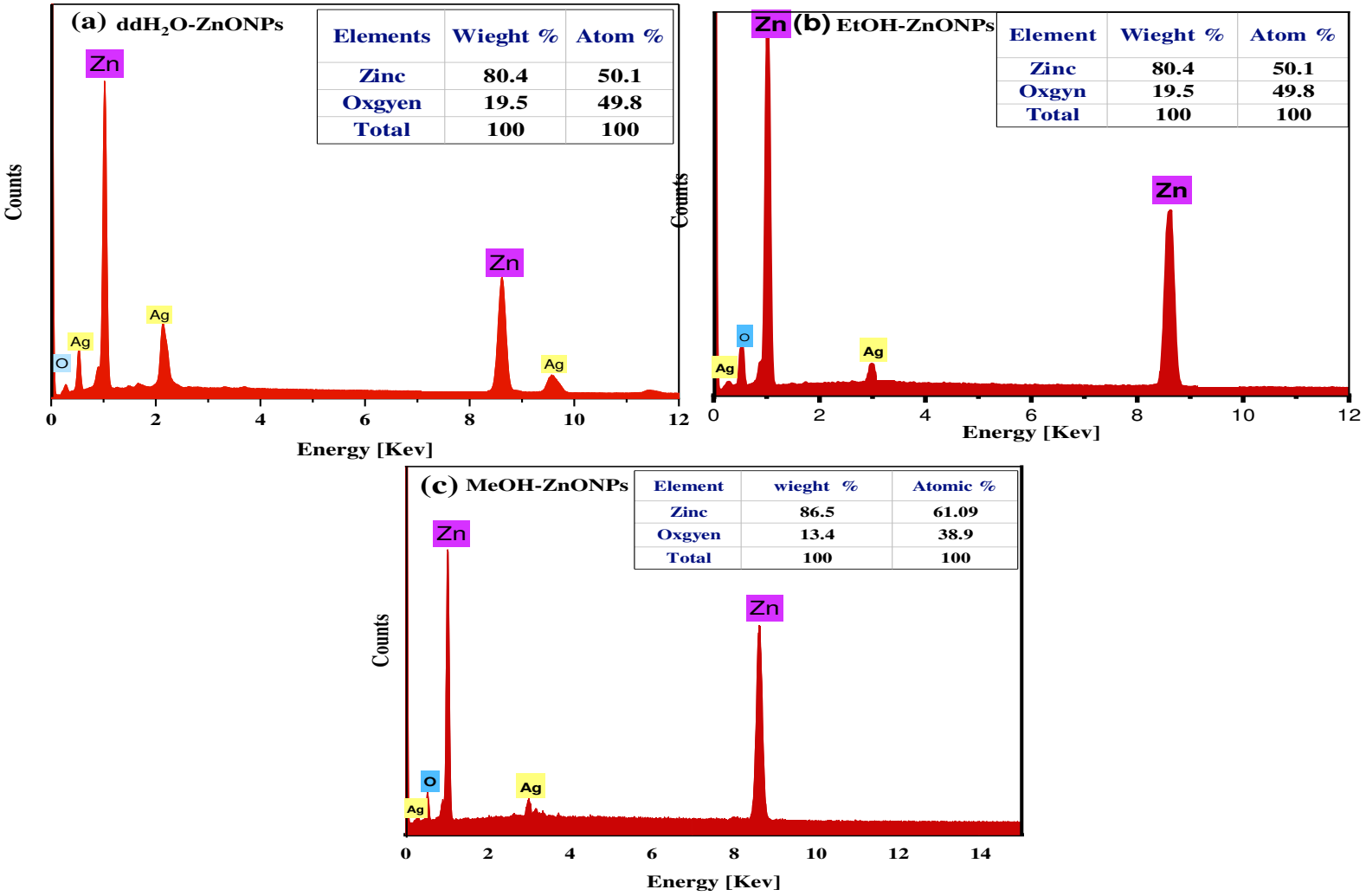

Figure 5. EDX spectrum of a) ddH_20-ZnO NPs; b) EtOH-ZnONPs; and c) MeOH-ZnONPs.

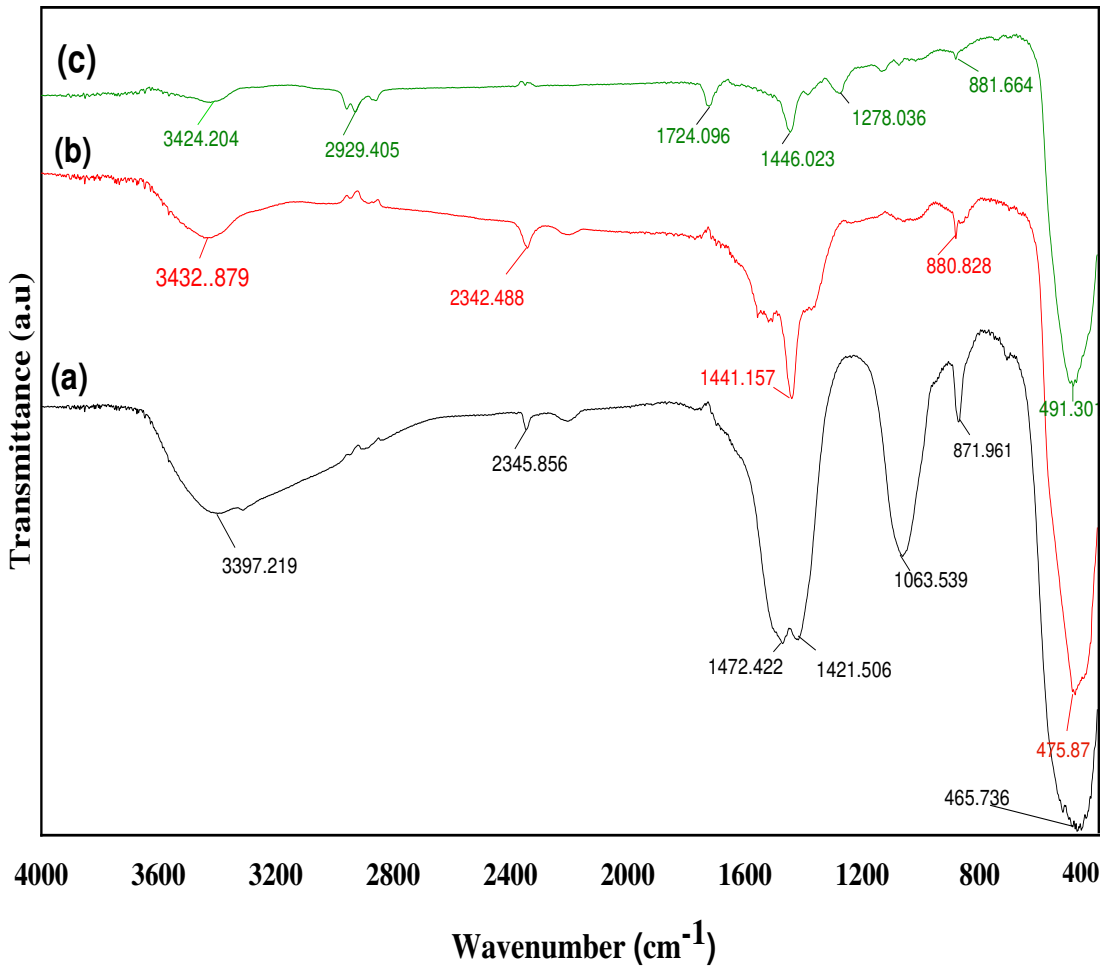

765

766 **Figure 6.** FTIR spectra of a) EtOH-ZnONPs; b) MeOH-ZnONPs; and c) ddH_2O-ZnONPs.

767

768

769

770

771

772

773

774

775

776

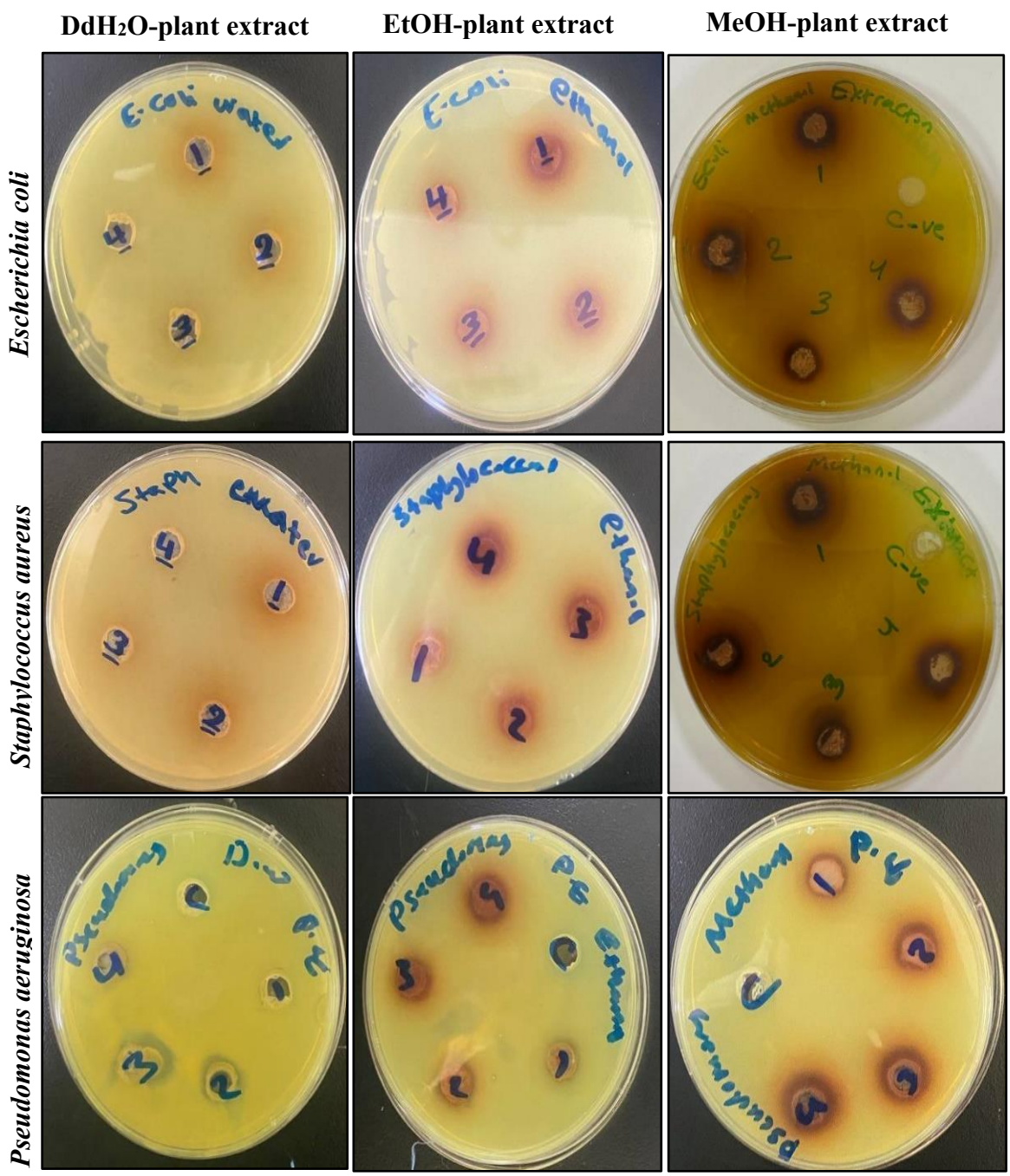

Figure 7. Anti-bacterial effects at different concentrations of WF seed extracted by three different solvents: ethanol, methanol, and double distilled water towards *S. aureus, E. coli, and P. aeruginosa* bacteria.

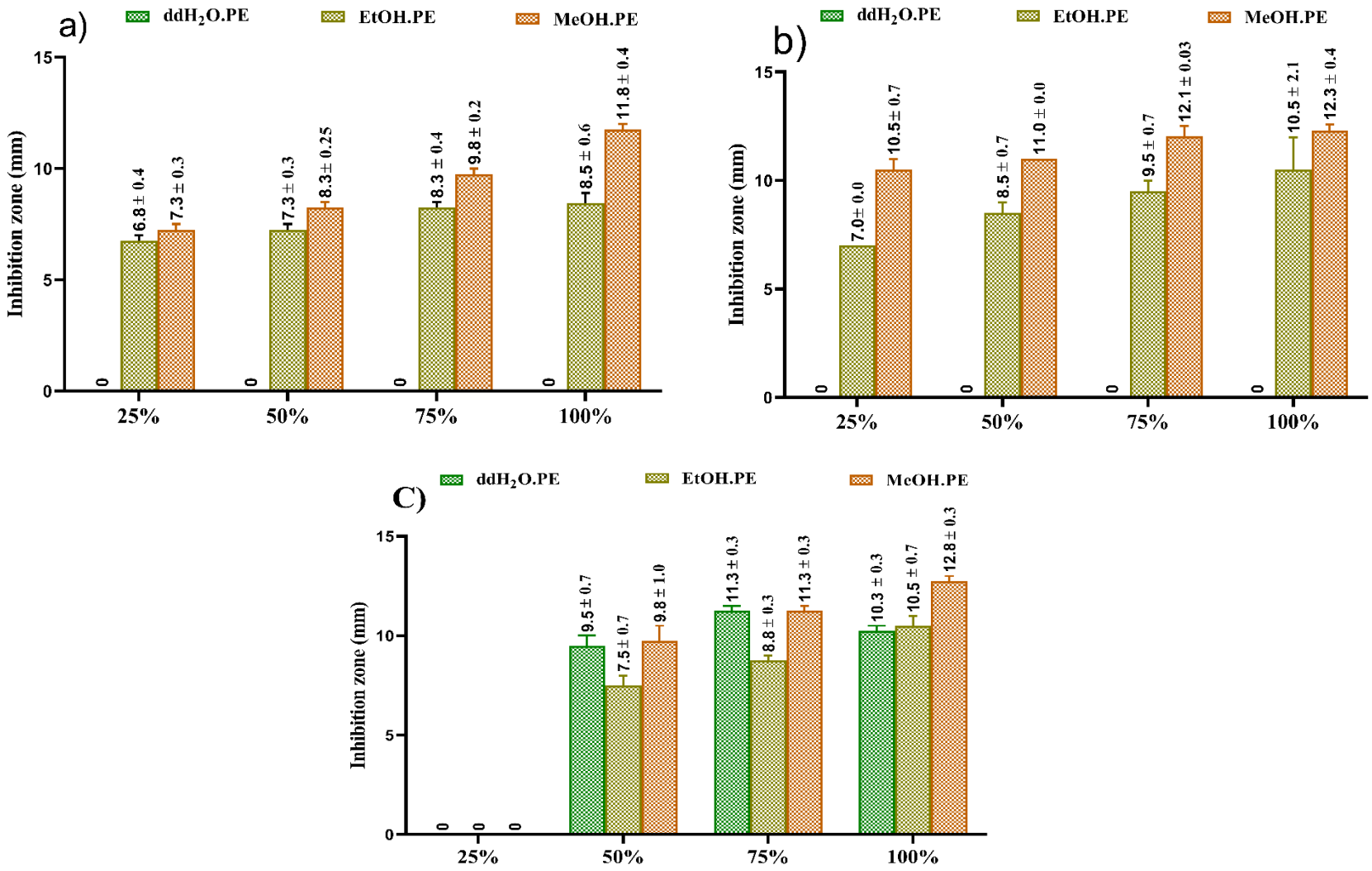

Figure 8. Anti-bacterial effects at different concentrations of WF seed extracted by a) double distilled water,b) ethanol, and c) methanol solvents towards *S. aureus, E. coli*, and *P. aeruginosa* bacteria

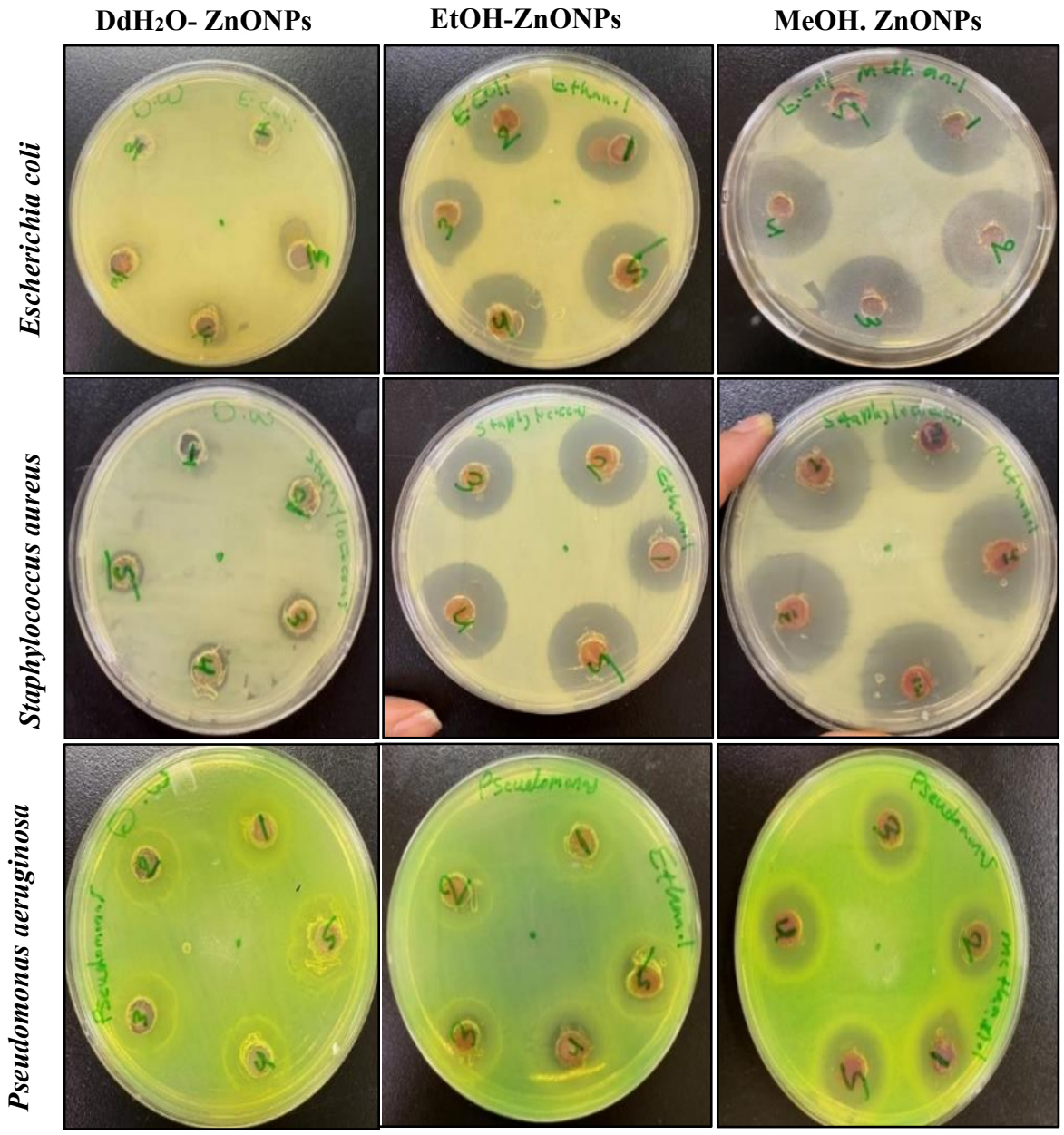

Figure 9. Anti-bacterial effects at different concentrations of ZnONPs prepared by plant extract in solvents: ethanol, methanol, and double distilled water towards *S. aureus, E. coli, and P. aeruginosa* bacteria.

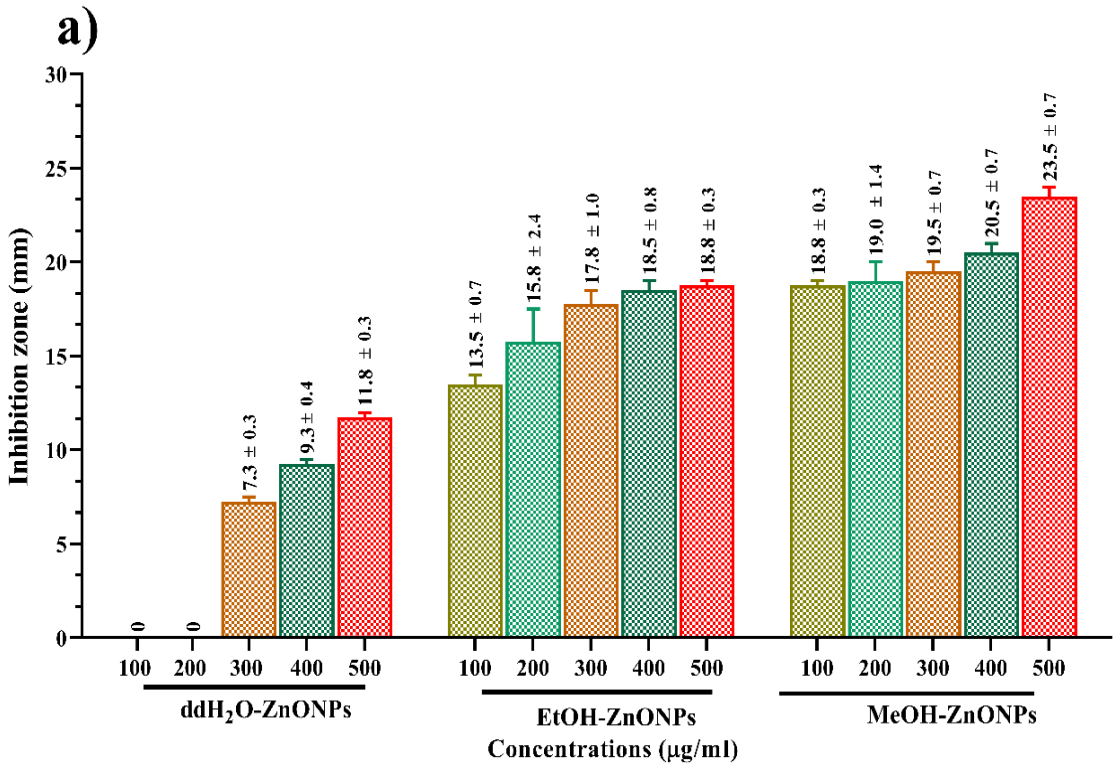
a)
Inhibition zone (mm)
0
5
10
15
20
25
30
0
0
7.3 ± 0.3
9.3 ± 0.4
11.8 ± 0.3
13.5 ± 0.7
15.8 ± 2.4
17.8 ± 1.0
18.5 ± 0.8
18.8 ± 0.3
18.8 ± 0.3
19.0 ± 1.4
19.5 ± 0.7
20.5 ± 0.7
23.5 ± 0.7
100 200 300 400 500
100 200 300 400 500
100 200 300 400 500
ddH2O-ZnONPs
EtOH-ZnONPs
MeOH-ZnONPs
Concentrations (µg/ml)

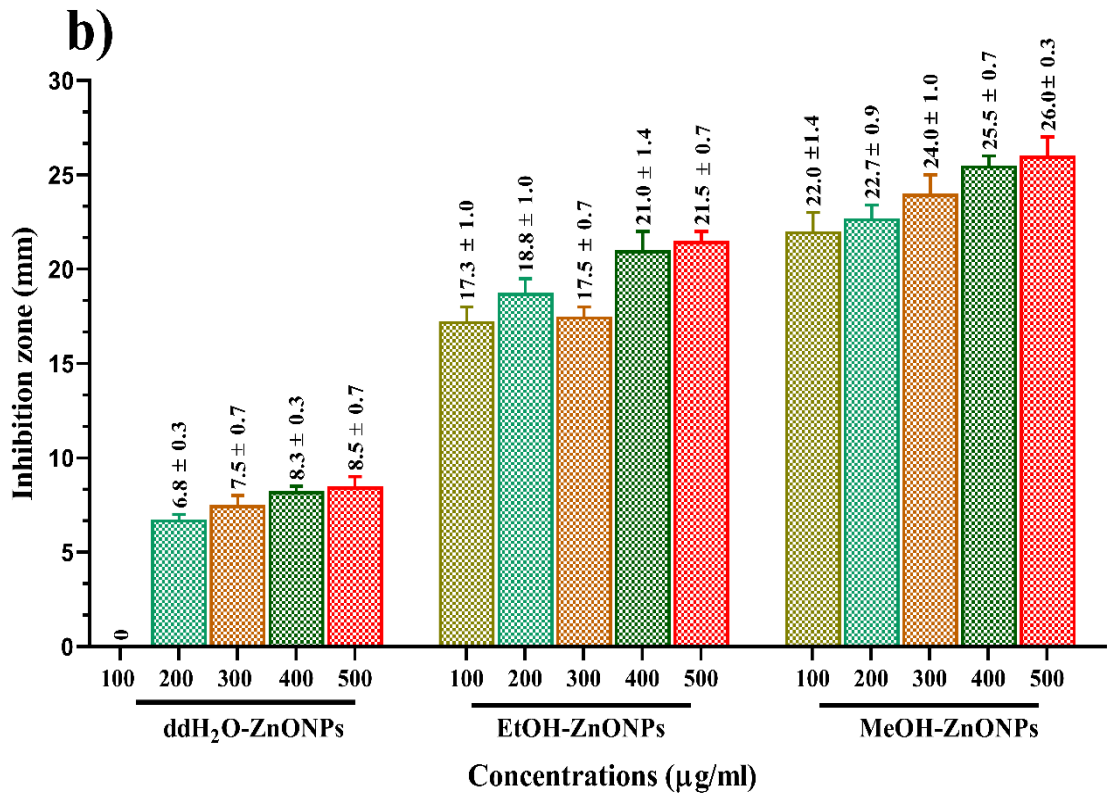
b)
Inhibition zone (mm)
0
5
10
15
20
25
30
0
6.8 ± 0.3
7.5 ± 0.7
8.3 ± 0.3
8.5 ± 0.7
17.3 ± 1.0
18.8 ± 1.0
17.5 ± 0.7
21.0 ± 1.4
21.5 ± 0.7
22.0 ±1.4
22.7± 0.9
24.0± 1.0
25.5 ± 0.7
26.0± 0.3
100 200 300 400 500
100 200 300 400 500
100 200 300 400 500
ddH2O-ZnONPs
EtOH-ZnONPs
MeOH-ZnONPs
Concentrations (µg/ml)

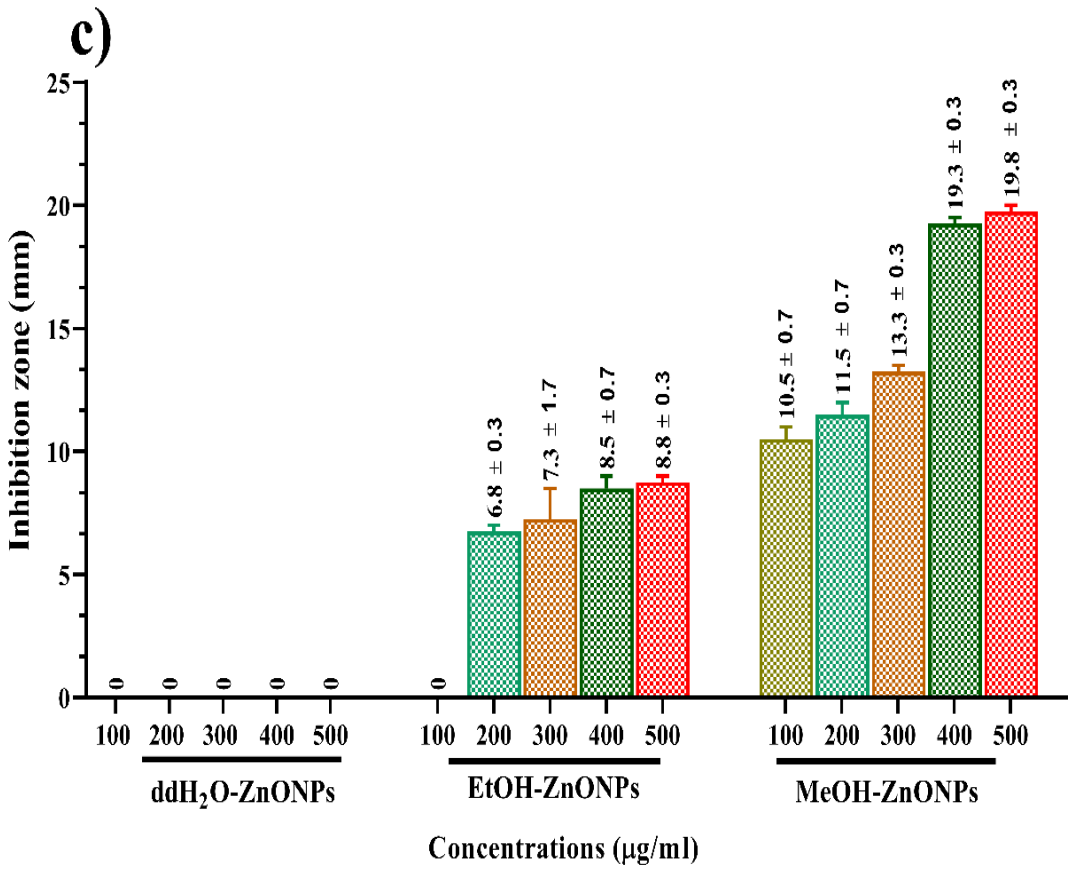

838 **Figure 10.** Anti-bacterial effects at different concentrations of WF seed extracted by solvents:
839 ethanol, methanol, and double distilled water towards *S. aureus, E. coli, and P. aeruginosa*
840 bacteria.

841

842

843

844

845

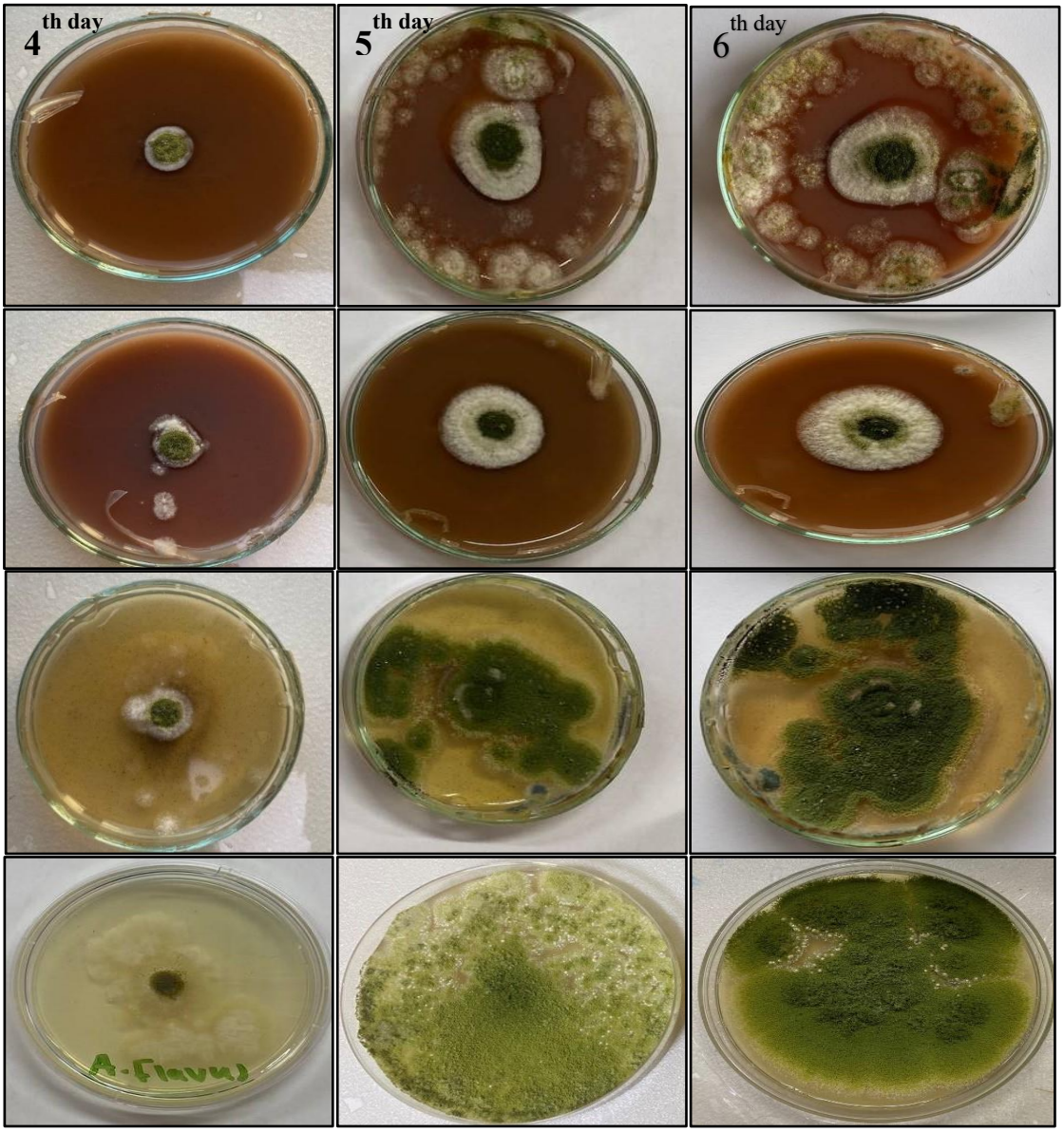

Figure 11. Macroscopic effect of ZnONPs prepared by ethanol, methanol, and double distilled water seed extract of *W. filarifia* against *A. flavus*.

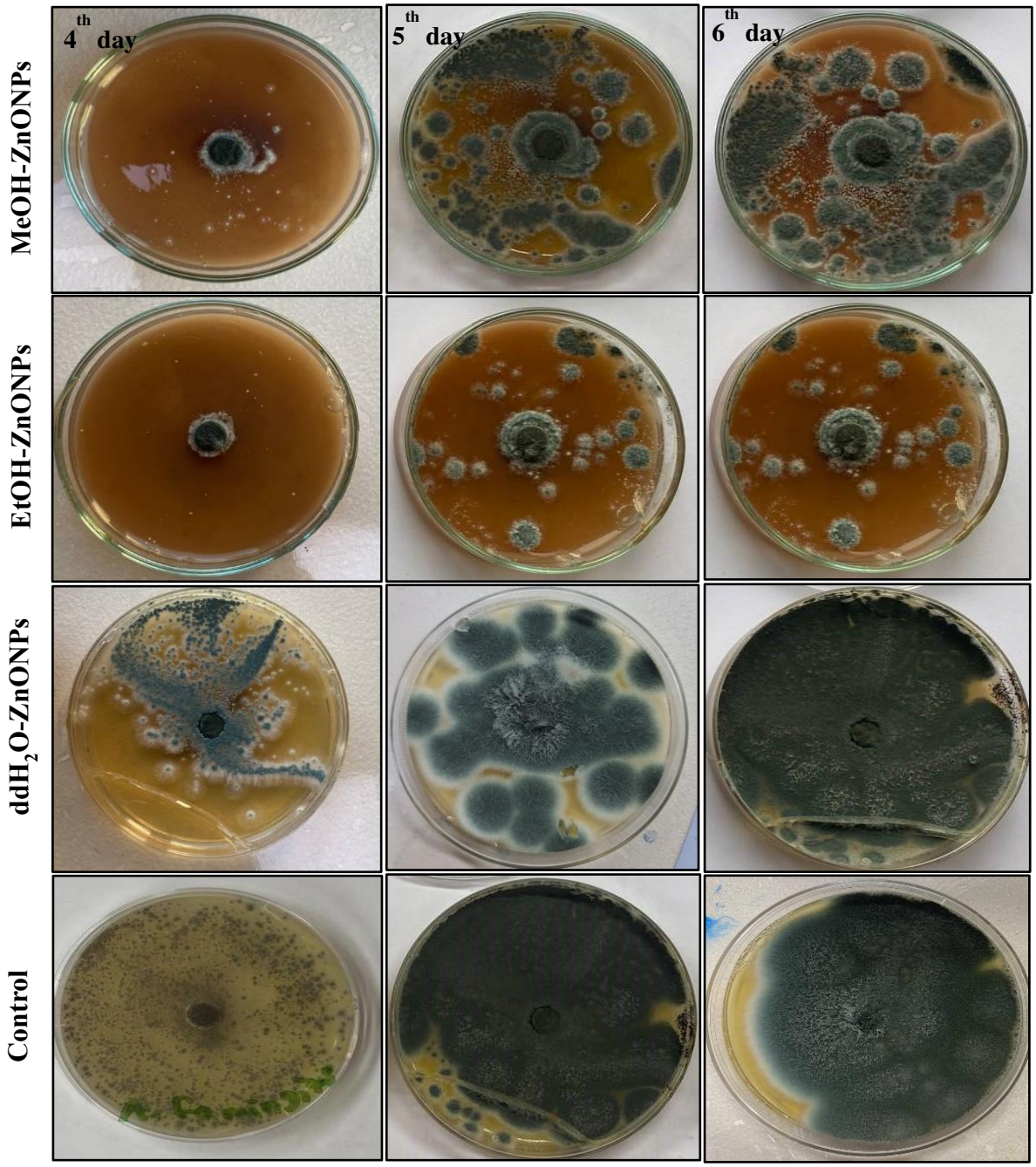

Figure 12. Macroscopic effect of ZnONPs prepared by ethanol, methanol, and double distilled water seed extract of *W. filarifia* against *A. fumigatus.*

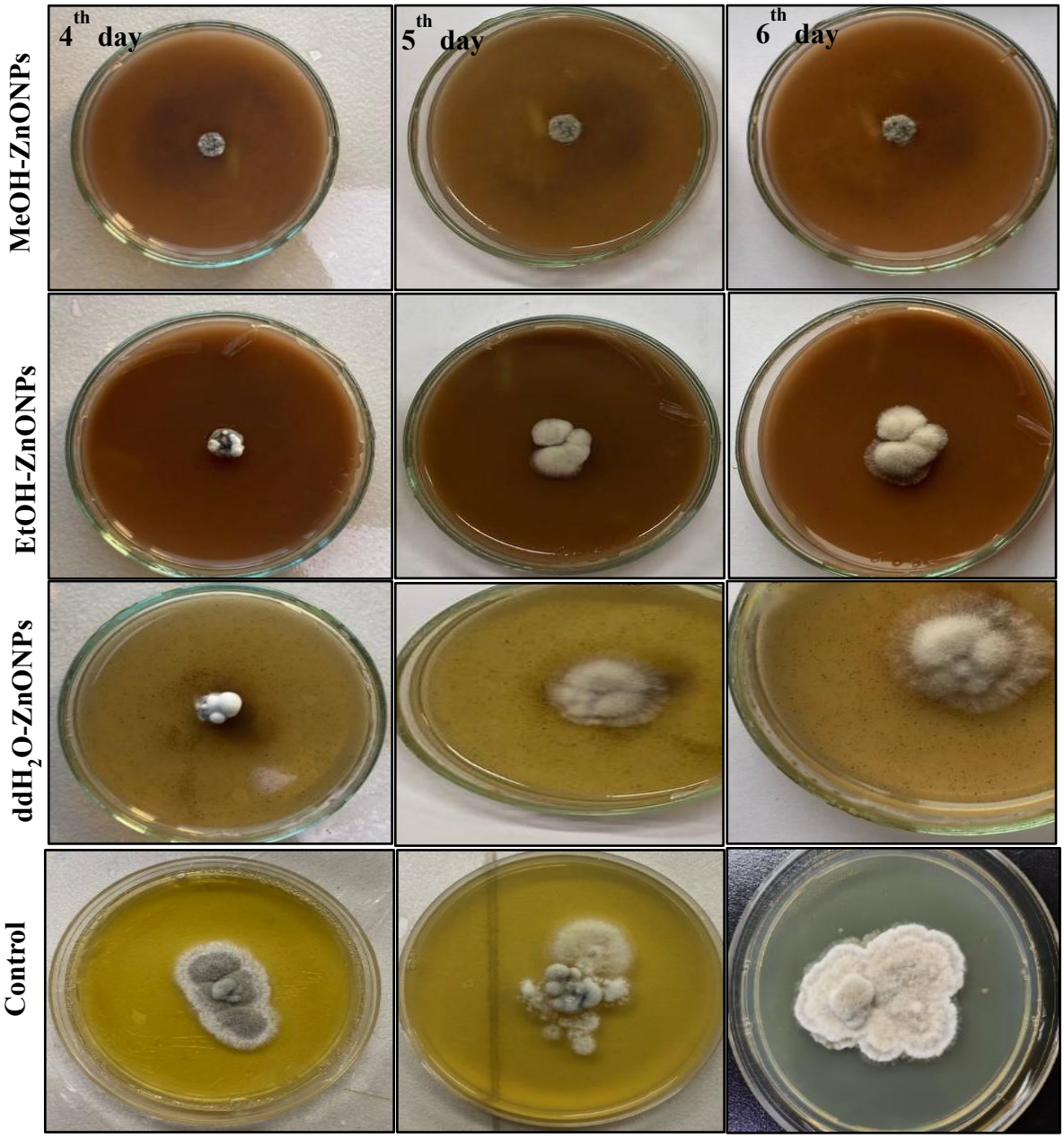

Figure 13. Macroscopic effect of ZnONPs prepared by ethanol, methanol, and double distilled water seed extract of *W. filarifia* against *S. apiospermum*.

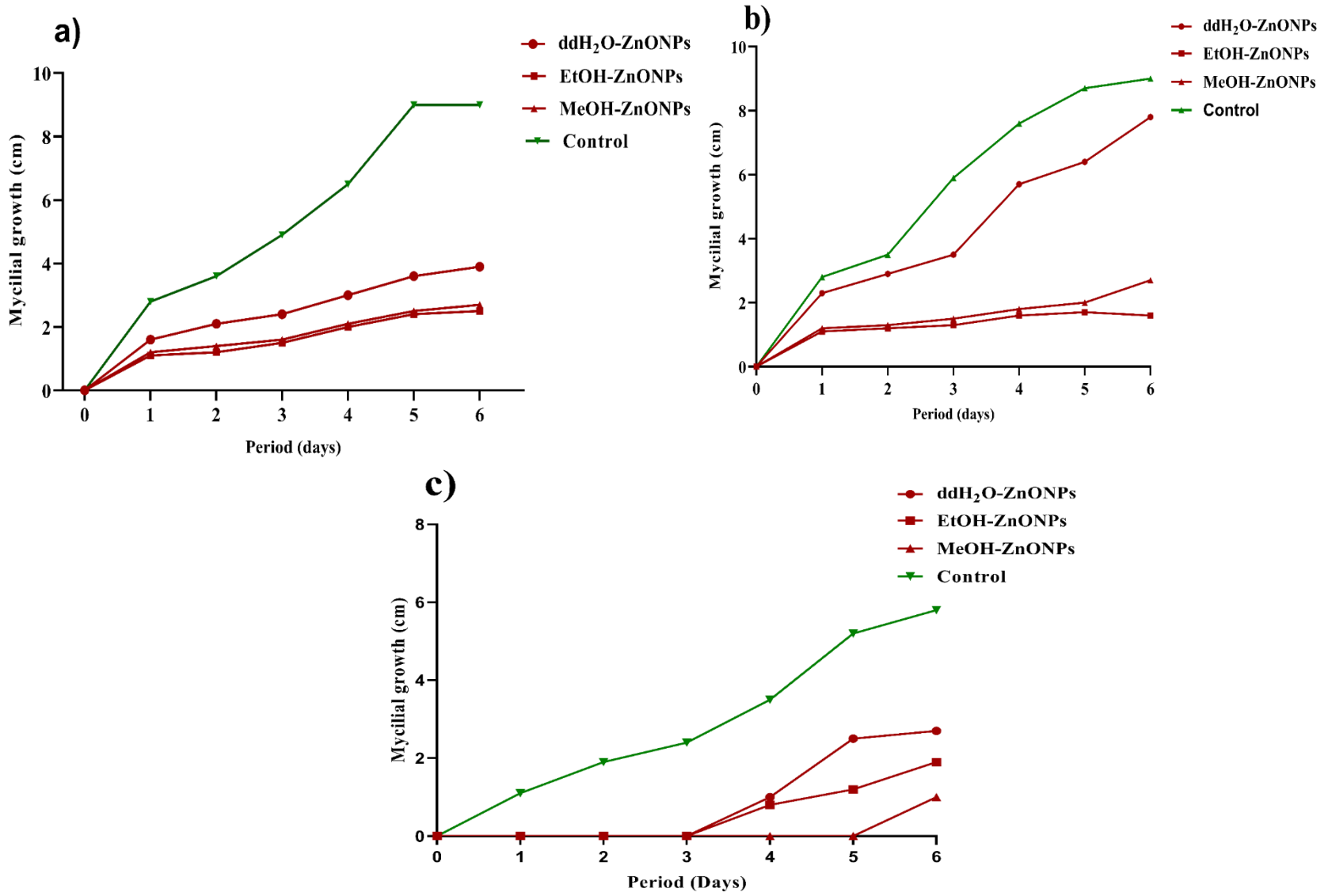

Figure 14. Anti-fungal results of a) *A. flavus,* b) *A. fumigatus, and c) S. apiospermum* treated with EtOH, MeOH ,ddH_2O-ZnONPs compared to control groups..

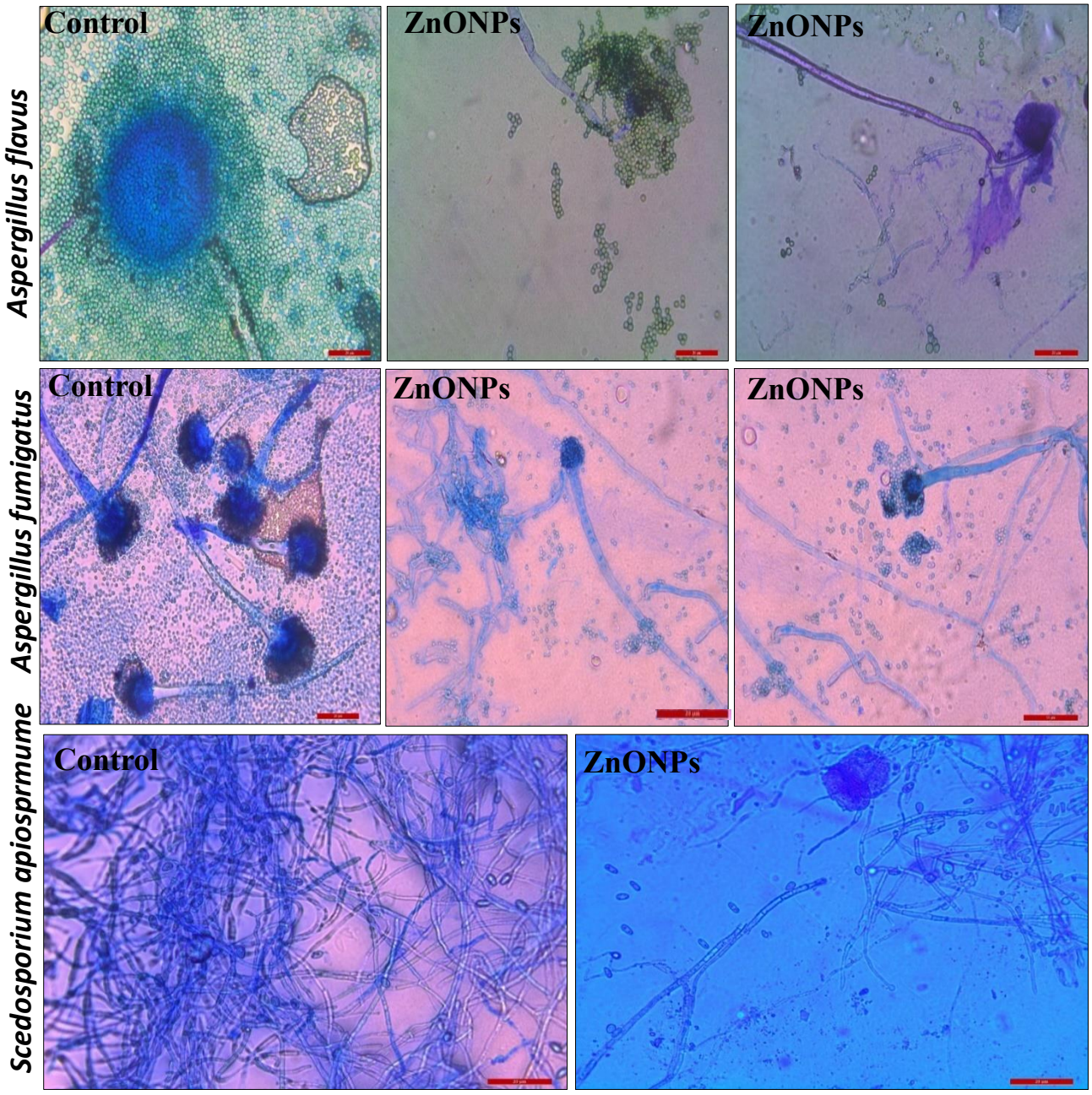

Figure 15. Microscopic effect of ZnONPs prepared by ethanol, methanol, and double distilled water seed extract of W. filarifia against A. flavus, A. niger, and S. apiospermum.

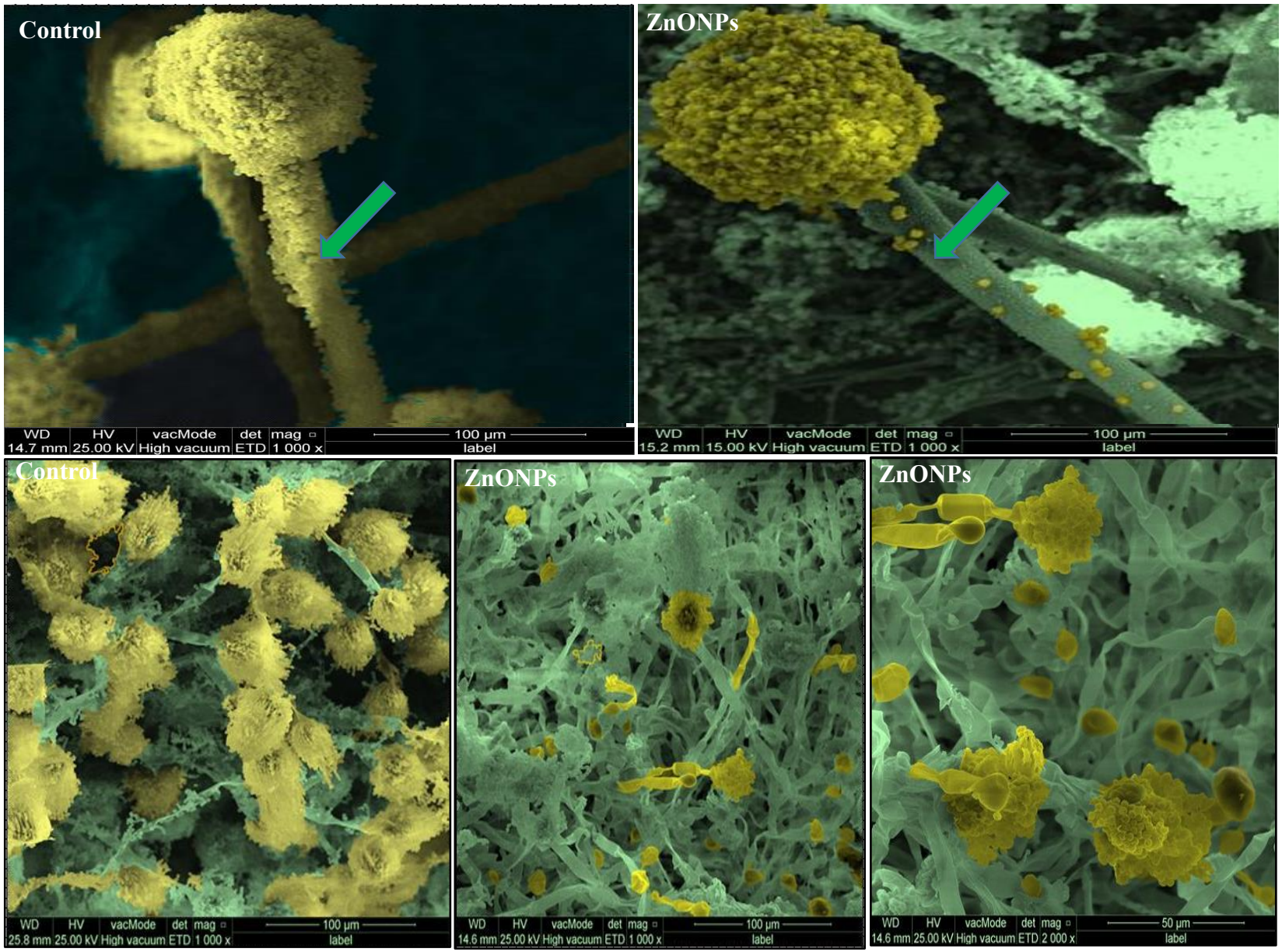
Aspergillus flavus
Control
WD 14.7 mm HV 25.00 kV vacMode High vacuum det ETD mag 1 000 x 100 µm label
ZnONPs
WD 15.2 mm HV 15.00 kV vacMode High vacuum det ETD mag 1 000 x 100 µm label
Aspergillus fumigatus
Control
WD 25.8 mm HV 25.00 kV vacMode High vacuum det ETD mag 1 000 x 100 µm label
ZnONPs
WD 14.6 mm HV 25.00 kV vacMode High vacuum det ETD mag 1 000 x 100 µm label
ZnONPs
WD 14.6 mm HV 25.00 kV vacMode High vacuum det ETD mag 2 000 x 50 µm label

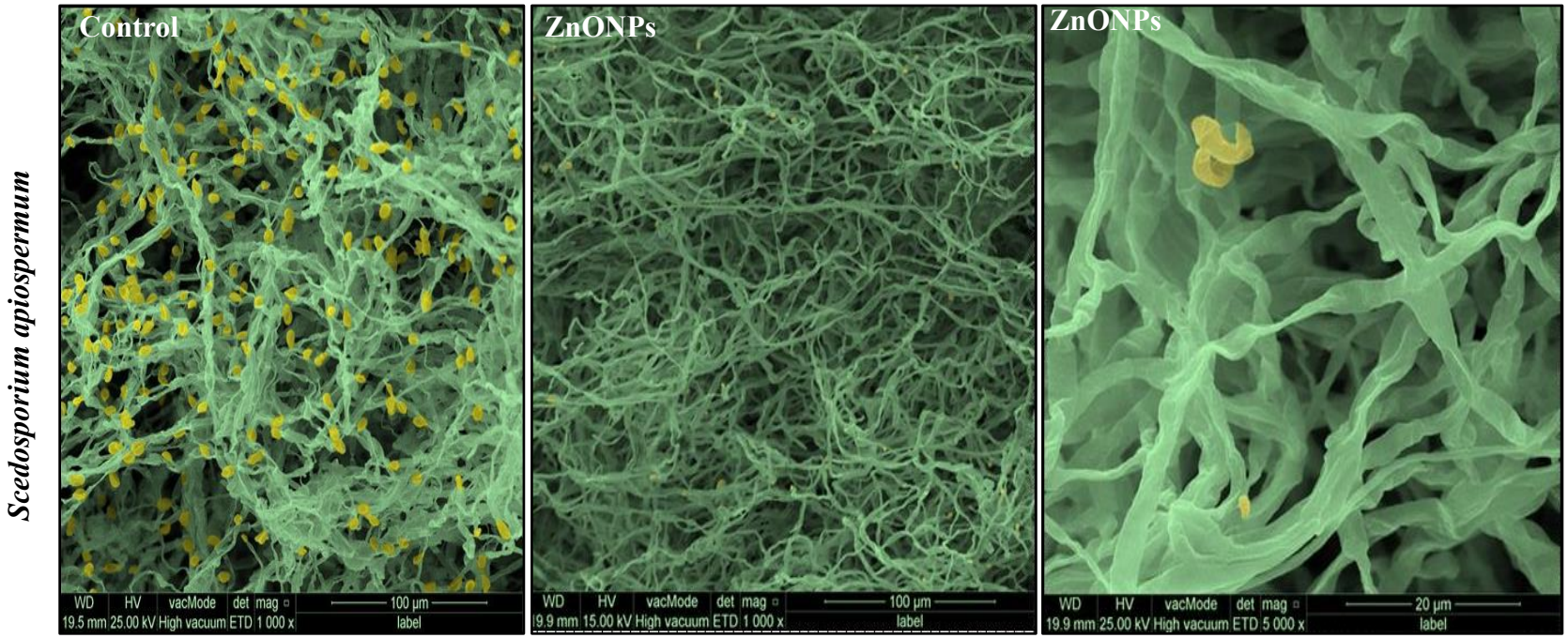

Figure 16. SEM images showing the morphology of *A. flavus, A. fumigatus,* and *S. apiospermum* treated with EtOH-ZnONPs and compared to control groups.

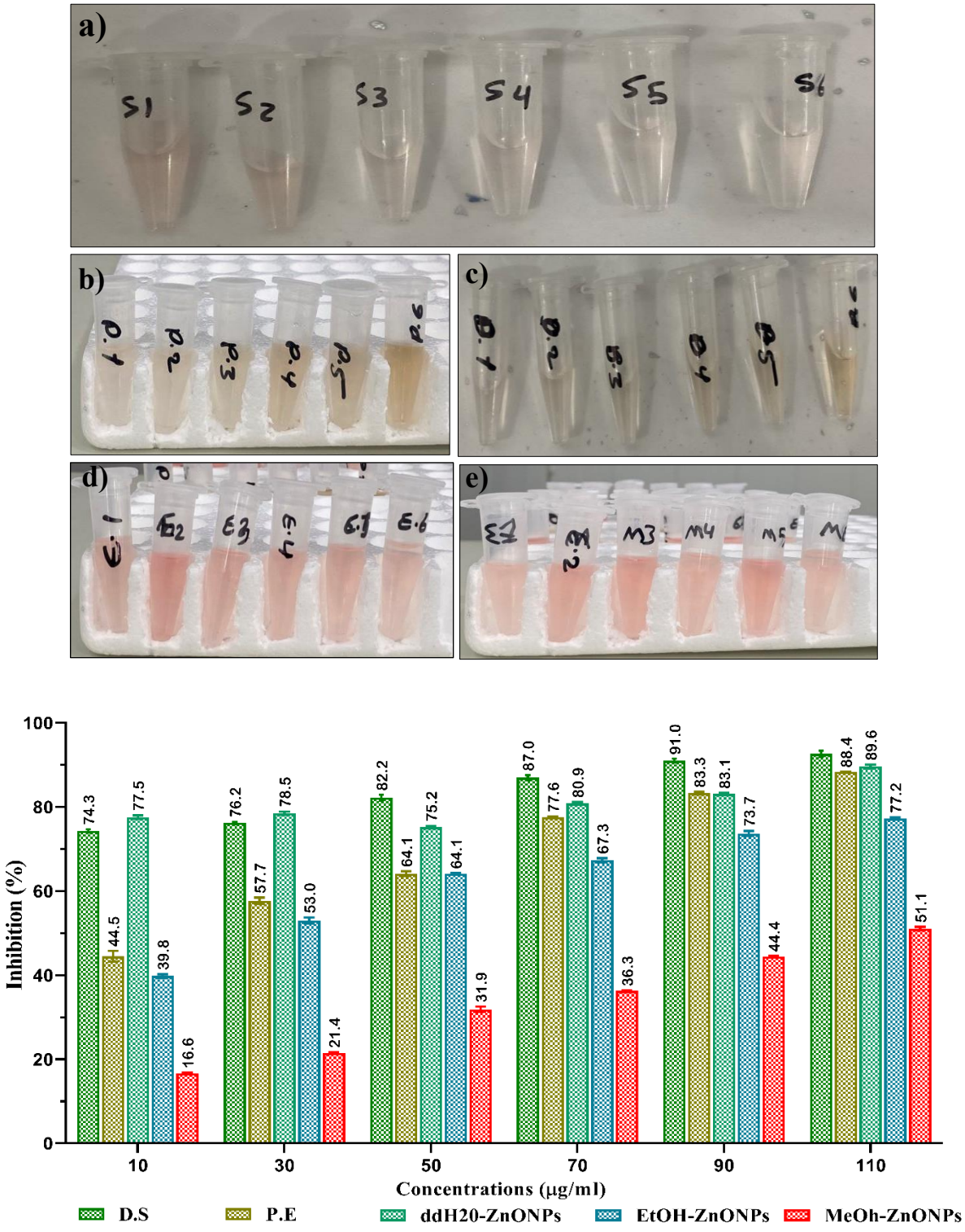

Figure 17. Anti-inflammatory analysis of a) standard drug, b) *W. filarifia palm* seed extract, and ddH2O, EtOH, and MeOH- ZnONPs.